NASA CONTRACTOR REPORT

NASA CR-1018

IMPROVEMENT AND OPTIMIZATION OF A MASS SPECTROMETER EMPLOYING A PHOTOIONIZATION SOURCE

by Walter P. Poschenrieder and Peter Warneck

Prepared by
GCA CORPORATION
Bedford, Mass.
for Langley Research Center

NATIONAL AERONAUTICS AND SPACE ADMINISTRATION • WASHINGTON, D. C. • MARCH 1968

NASA CR-1018

IMPROVEMENT AND OPTIMIZATION OF A MASS SPECTROMETER EMPLOYING A PHOTOIONIZATION SOURCE

By Walter P. Poschenrieder and Peter Warneck

Issued by Originator as Report No. GCA-TR-67-12-N

Prepared under Contract No. NAS 1-6335 by
GCA CORPORATION
Bedford, Mass.

for Langley Research Center

NATIONAL AERONAUTICS AND SPACE ADMINISTRATION

For sale by the Clearinghouse for Federal Scientific and Technical Information
Springfield, Virginia 22151 – CFSTI price $3.00

TABLE OF CONTENTS

IMPROVEMENT AND OPTIMIZATION OF A MASS SPECTROMETER EMPLOYING A PHOTOIONIZATION SOURCE

by Walter P. Poschenrieder and Peter Warneck

SUMMARY

This report describes further improvements of the photoionization mass spectrometer, originally developed under Contract NAS1-4927. The experiments performed under that contract showed the basic feasibility of analytical photoionization mass spectrometry. At the same time, certain limitations were indicated, particularly with regard to the discrimination of ions with different ionization potentials and coinciding mass numbers, e.g., CO and N_2. This limitation could be traced back to two main sources: namely, the second and higher order uv spectrum produced by the grating, and uv light scattering in the monochromator. A considerable improvement has been achieved by the use of uv filters which reduce the intensity of the higher order spectrum and scattering by about two orders of magnitude. Accordingly, the detection limit for CO in N_2 was improved from 5000 to 100 ppm. The performance of a thin-metal indium filter was compared with an argon gas filter and the latter was found to be the better choice since:

(a) The gas filter is simple and rugged while the thin-metal filter is very fragile.

(b) Within its transmission range, the gas filter provides practically 100 percent transmission while a thin-metal filter achieves only about 10 percent.

(c) The gas filter is more versatile since the filter characteristic can be easily and quickly changed by the use of different gases.

With a basic sensitivity in the 10-ppm range and a discrimination power of better than 100 ppm for gases with interfering mass peaks, the photoionization mass spectrometer represents an analytical tool of unique capabilities and great potential.

The following table lists the investigated gas mixtures and the detection limits which were found.

Wavelength Å	Light Source	Gas Mixture	Interfering Mass Number	Detection Limit
923	N_2 spark source + argon filter	0.1% N_2O in CO_2	44	500 ppm N_2O
879	argon spark source argon filter	0.05% CO in N_2	28	100 ppm CO
879	argon spark source argon filter	0.1% C_2H_4 0.19% CO in N_2	28	50 ppm C_2H_4 from M 26
1216	argon-hydrogen dc source CO_2 filter	0.17% acetone in butane	58	100 ppm acetone

INTRODUCTION

A detailed description of the historical development and the basic principle of photoionization mass spectrometry is in the Final Report of Contract No. NAS1-4927 [1]* which directly preceeded the present contract. Therefore, a brief recapitulation of the basic problems and the operating principles of instrument will be sufficient.

Mass determination by static or dynamic electric and magnetic fields necessitates the ionization of the atoms or molecules of interest. Ionization can be achieved in various ways, e.g., by electron or ion impact, by high temperatures, by high electric fields, and also by photoionization. Many different ion sources known use one or the other, or sometimes a combination of these principles, but so far, photoionization has found only very limited application in analytical mass spectrometry. Most work in this field rather dealt with the investigation of photoionization phenomena themselves.

All the different methods of ionization have certain advantages and disadvantages and none can claim universality. Those methods which provide a high degree of ionization also produce complex spectra because the molecules are not only ionized but also dissociated. It is a well-known fact that for electron impact ion sources produce very complex spectra from high molecular gases and vapors. Interpretation of these spectra becomes very complicated for mixtures of such gases because the superposition of the individual cracking patterns causes multiple interferences. Field ionization and photoionization, on the other hand, produce only little fragmentation; therefore, the spectra are much simpler. Both these methods share the common disadvantage of a much lower ionization rate. This low ionization rate, however, is not due to a poor ionization mechanism itself, but is merely caused by limitations in other parameters involved. In the field emission source, the volume with sufficiently

*Numbers in [ ] throughout text indicate reference numbers.

high field strength is very small, and in the photoionization source, the number of photons which can be produced by the most efficient uv light sources yet known is not as high as the number of electrons easily obtained from a hot filament or other electron sources.

Sufficient ion production becomes even more problematic if photoionization with dispersed uv radiation is used. (Dispersed radiation results when a uv monochromator is switched between uv light source and ion source.) This appears to be rather unfortunate since photoionization with dispersed uv clearly offers some unique features which would be of great value in analytical mass spectrometry. Using a monochromator, it is possible to set the energy of the ionizing photons with an accuracy of at least 0.01 eV; thus a degree of discriminative ionization can be achieved which is hardly feasible with any of the other methods.

In principle, a similar result could be obtained by using a beam of monoenergetic electrons. Practical application is hampered by intensity problems for electron beams with an energy spread of less than 0.5 eV in the total energy region 5 to 20 eV. Even more restrictive is the very low differential ionization of gases under electron impact at electron energies close to the ionization threshold. Photoionization, in contrast, yields a particularly high ionization cross section near the threshold. Indeed, a quantitative comparison of both methods, considering the present state-of-the-art and also basic limitations, shows a significant superiority of photoionization as long as ionizing energies close to the ionization threshold are involved. Furthermore, such studies also indicate that sufficient sensitivity for gas analysis by selective photoionization might well be attained, provided all means of technology are utilized.

With this in mind, a photoionization mass spectrometer was developed with the following features:

(1) A low pressure ceramic capillary spark source delivering the most intense multi-line uv spectrum which can be obtained presently.

(2) A focusing 1/2-m Seya Monochromator of large solid angle acceptance with a gold or platinum plated 1200 lines/mm replica grating.

(3) A specially design ion source which permits sample gas pressures up to 20 μ without loss in linearity and which produces a minimum of ion-molecule reactions. (Ion-molecule reactions could lead to the formation and ionization of unwanted species.)

(4) A special mass spectrometer with a transmission in excess of 10 percent with stigmatic focusing and absence of image aberrations up to the fourth order.

(5) A high gain, low noise multiplier used as the ion detector and equipped with a special ion suppressor with a particularly sharp cut-off characteristic to permit the rejection of all ions which have undergone secondary reactions or have been produced by such reactions.

(6) A powerful vacuum system with a total baffled pump speed of 750ℓ/sec with differential pumping that provides independence of the pressures in the light source, monochromator, ion source, and mass spectrometer. With this system, a high pressure can be maintained in the light source and ion source without detrimental effects to the performance of the monochromator or mass spectrometer.

The experimental results which were obtained with this photoionization mass spectrometer confirmed the practicality of the approach. The sensitivity of the instrument was sufficient to detect gas traces in the 10-ppm range. When discriminative ionization was used, 100 ppm of CH_4 in O_2 at M = 16 and 0.5 percent of CO in N_2 at M = 28 could be detected.

A detection limit of 0.5 percent CO in N_2 was still somewhat disappointing, particularly for an application where at least the toxicity level of 100 ppm of CO in air should be detectable. The experiments, however, also indicated the sources of this limitation: namely, (a) interference between the first and higher order spectrum as produced by the monochromator grating, and (b) uv scattering in the monochromator. By a careful baffling of the light beam, it is possible to keep uv scattering in the monochromator at a minimum, but irregularities (blisters and dust) of the grating will set a limit. The production of higher order spectra is an inherent property of a diffraction grating which is often deliberately used to gain higher resolution. In the present application, however, the transmission of higher order lines superimposed onto the first order spectrum can still cause considerable ionization of atoms or molecules with ionization energies above the selected first order photon energy. No technical uv gratings which only or preferentially produce a first order spectrum are known; thus it is obvious that some other means have to be found to avoid the simultaneous transmission of higher order lines.

The laws of diffraction show that all wavelengths which are multiple fractions of a certain first order wavelength appear under the same diffraction angle as higher orders. In the case of CO in N_2, a strong line at 835Å was used which should ionize CO only; but some N_2 was still ionized by a line at 419Å. This line appears in second order at 838Å, and the resolution of the monochromator was not high enough to separate 838 and 835Å sufficiently.

From the foregoing, it is evident that a solution of the uv interference problem requires some additional means. One possibility is to prevent or minimize the emission of uv radiation at and below half of the actually required wavelength right in the light source or to suppress such unwanted wavelengths somewhere between light source and ion source by use of a filter. The efforts which were taken and their results are discussed in the following section.

UV FILTERS AND LIGHT SOURCES

Filtering in the uv region below 1000Å is based on the selective absorption of thin metallic films and of gases. Between 1000 and 1500Å, compact solids such as lithium fluoride or sapphire provide a sharp cutoff toward the shorter wavelengths. Above 1500Å, interference filters are in use; but at shorter wavelengths, technological difficulties arise. In this project, only the presence of short wavelengths is harmful and the use of a filter with a short wavelength cutoff is sufficient. In addition, a cutoff in the range below 1000Å is required in most cases; therefore, the discussion will be restricted to the use of thin-metal and gas filters.

Thin-Metal Filters

The application of thin-metallic filters for the vacuum uv region is a comparatively new field and the amount of data is still limited. A compendium of the present knowledge was given by W. R. Hunter, O. W. Angel and R. Tousey [2]. Figures 1 and 2 are taken from this reference. Figure 1 is a summary diagram of the transmission of the materials so far investigated. The transmission is plotted vertically: the straight horizontal lines denote undetectable small transmission. The x-ray edges are shown as steps and the arrowheads show the critical wavelengths; dotted sections indicate ranges which are based on calculations only. From Figure 1 it can be seen that most filter metals are not suitable for suppressing the second and higher order spectrum which would interfere with the first order spectrum in the range of main interest from 800 to 1200Å. It is evident that for this purpose, the filter should have zero transmittance from at least 600Å downward. Minimization of stray light interferences, however, necessitates the even more stringent condition; the cutoff must be as close as possible to the range of selected ionization wavelengths. For the discrimination of CO and N_2, for example, the following considerations apply: The ionization threshold of N_2 lies at 795Å while CO will be ionized up to 885Å; thus, if both gases have to be detected in the presence of each other, a filter with a cutoff directly below 795Å would be ideal. If only CO were of interest, a cutoff closer to 885Å would be even better, since any residual ionization of N_2 by stray light or higher order would then be completely eliminated.

From all the metals given in Figure 1, only the transmission characteristics of indium come close to the requirements stated above. Figure 2 shows the transmittance of two indium films of different thicknesses in more detail. It is seen that indium has a rather sharp cutoff at about 750Å and a fairly good transmission between 800 and 900Å. Since above 1000Å the transmittance again becomes poor, the application of the indium filter is limited to the range between 800 and 1000Å, corresponding to ionization energies from 15.6 to 12.5 eV. Figure 1 also indicates increasing transmittance of indium below 150Å, but the intensities of the uv spark source below 400Å are low and, therefore, any interference from this range is negligible. All the other thin-metal filters listed in Figure 1 seem not

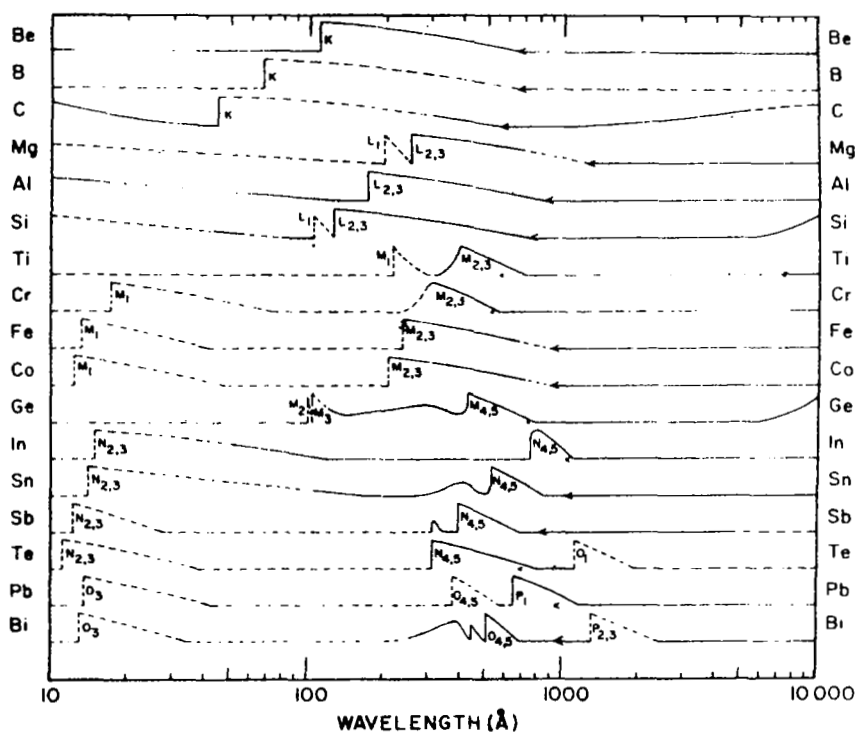

Figure 1. Schematic of transmission properties of various thin films.

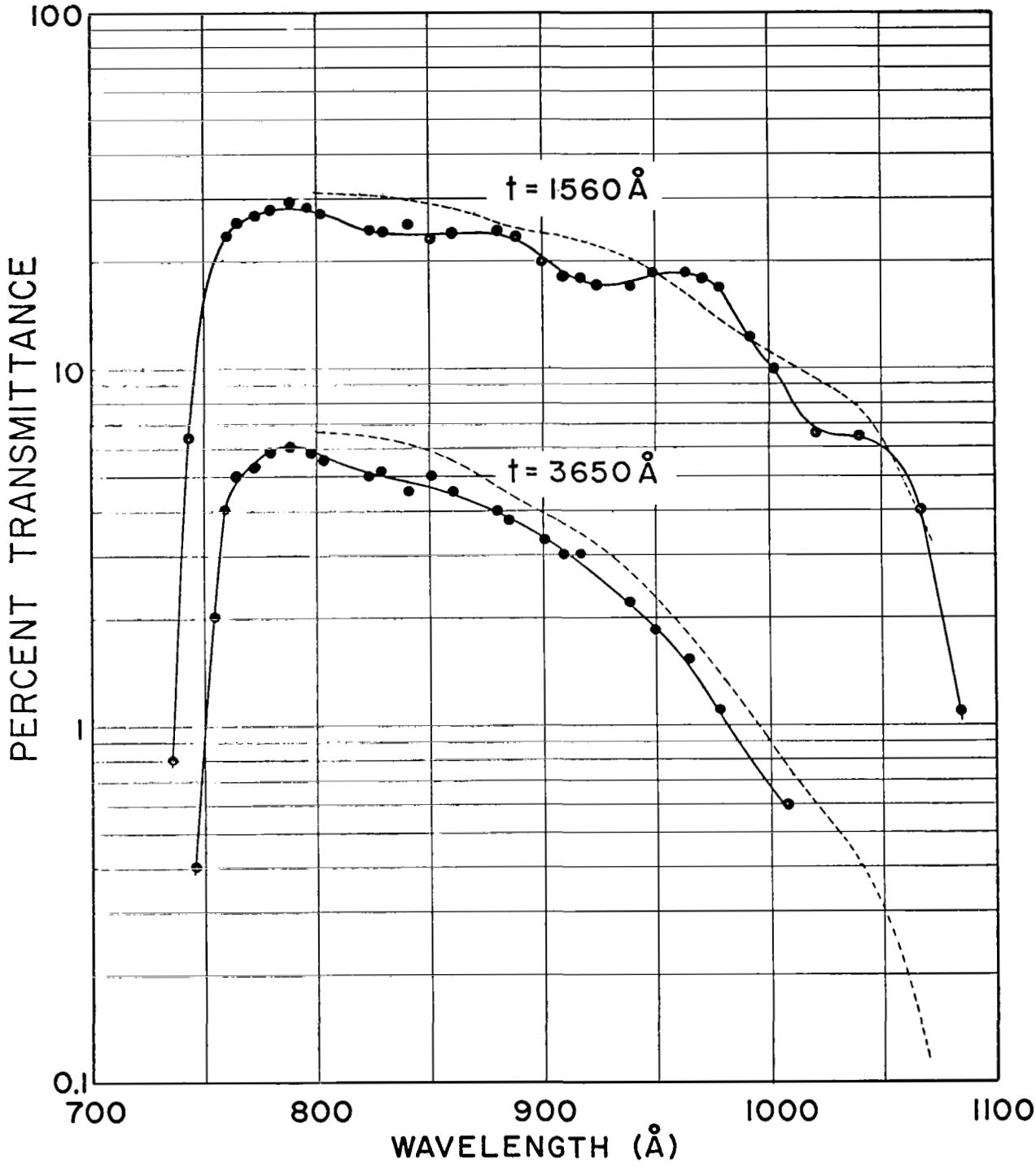

Figure 2. Transmittance of indium films. Dashed lines are calculated values.

to be useful in the intended application, since the cutoff wavelengths either are too low or are followed by an additional range of transmittance at about half of the wavelength.

Gas Filters

In contrast to the very delicate thin metal filter, the gas filter is a very rugged arrangement. In addition, as will be shown in the following, they provide more versatility than thin-film filters and are very easy to handle. Changing the gas pressure can change filter density and mixing different gases will give a variety of different characteristics.

As with the application of thin-film filters in the uv, the practical use of gas filters for the vacuum uv is a recent development. Nevertheless, the absorption cross sections in the vacuum uv range of many gases are now known and a good deal of this information is in the literature [3,4].

Figures 3 through 7 show the absorption characteristics of the various rare gases. It is seen that the cutoffs of these gases from about 500Å for He to 1020Å for Xe covers a good part of the range of main interest. With the exception of He, the absorption continuum is directly preceeded by a range with a number of strong discrete absorption lines which are caused by autoionization. This range is only 2Å in the case of Ne but increases with the number of electron shells and becomes as wide as 100Å for Xe. This behavior has no appreciable effect in the considered application, since the absorption between the lines is still high. In addition, the average absorption over the range of autoionization is at least as high as in the following continuum.

The behavior of the absorption characteristic toward shorter wavelengths differs considerably for the different gases. Figure 8 shows the relative absorption characteristics for all rare gases in one graph. One can see that Xe has the highest absorption of all the rare gases, but the absorption drops fast toward shorter wavelengths. The absorption of Ar increases at first with decreasing wavelengths, and Ar also has the highest absorption of all the gases between 600 and 400Å. From Figure 8, it is obvious that the addition of Ar to Xe can compensate for the loss of absorption below 600Å and thus reduce possible second order interferences. As already discussed in connection with thin-metal filters, lack of high absorption below 400Å is not critical because of the weakness of the light source spectrum in this range.

The absorption characteristic of Ar seems to be ideally suited for the specific problem of CO detection in N_2. The cutoff of Ar (788Å) lies very close to the ionization onset of N_2 at 795Å; therefore, detection of N_2 is still possible with the filter applied but second order interferences and short wavelength scattering is drastically reduced.

The rare gases show particularly simple spectra owing to their mono-atomic structure. In contrast, the spectra of molecular gases have a much stronger structure because of the possibility of vibrational and rotational energy levels.

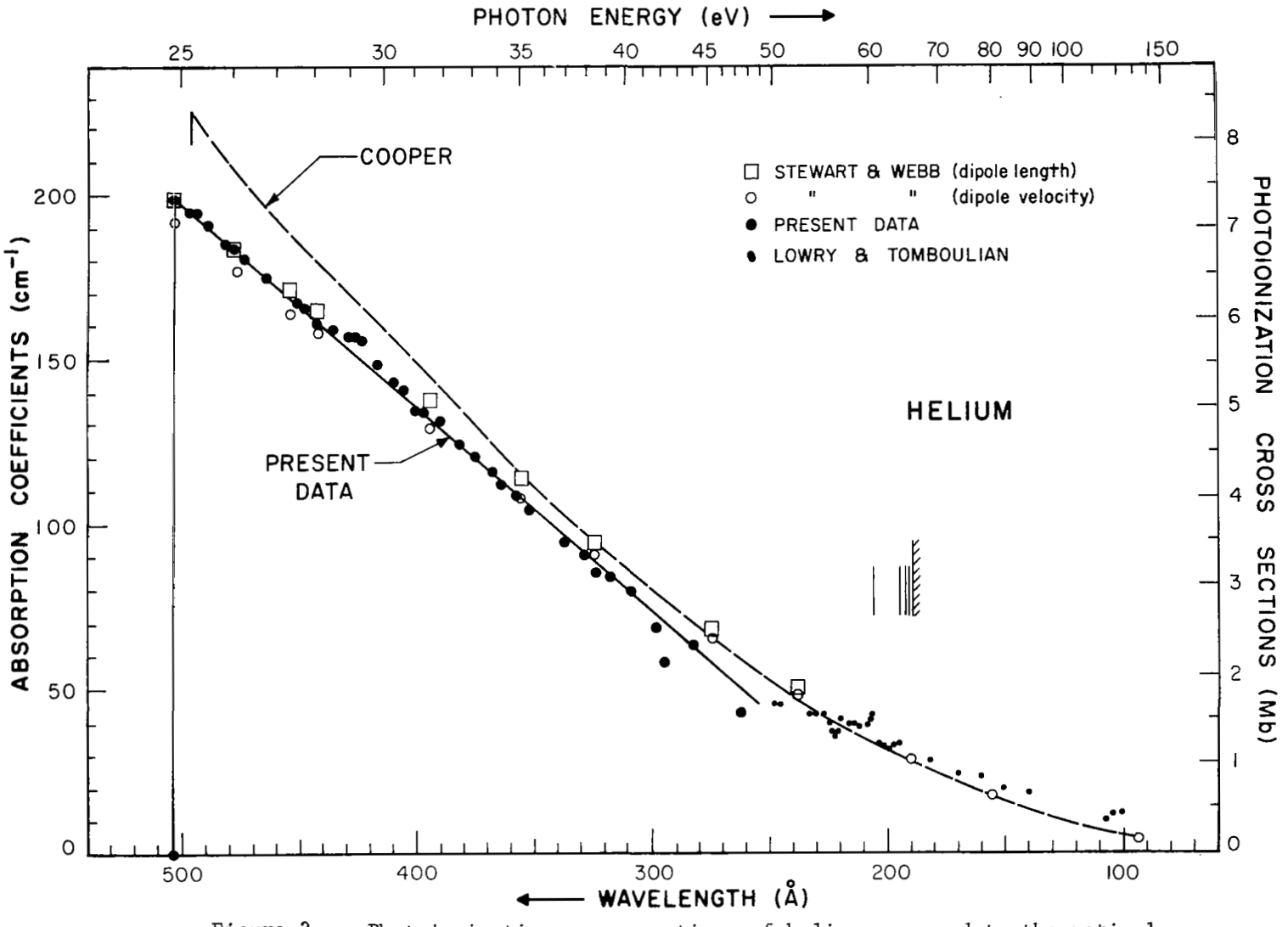

Figure 3. Photoionization cross sections of helium compared to theoretical values. The vertical lines indicate the position of discrete absorption lines due to double electron excitations.

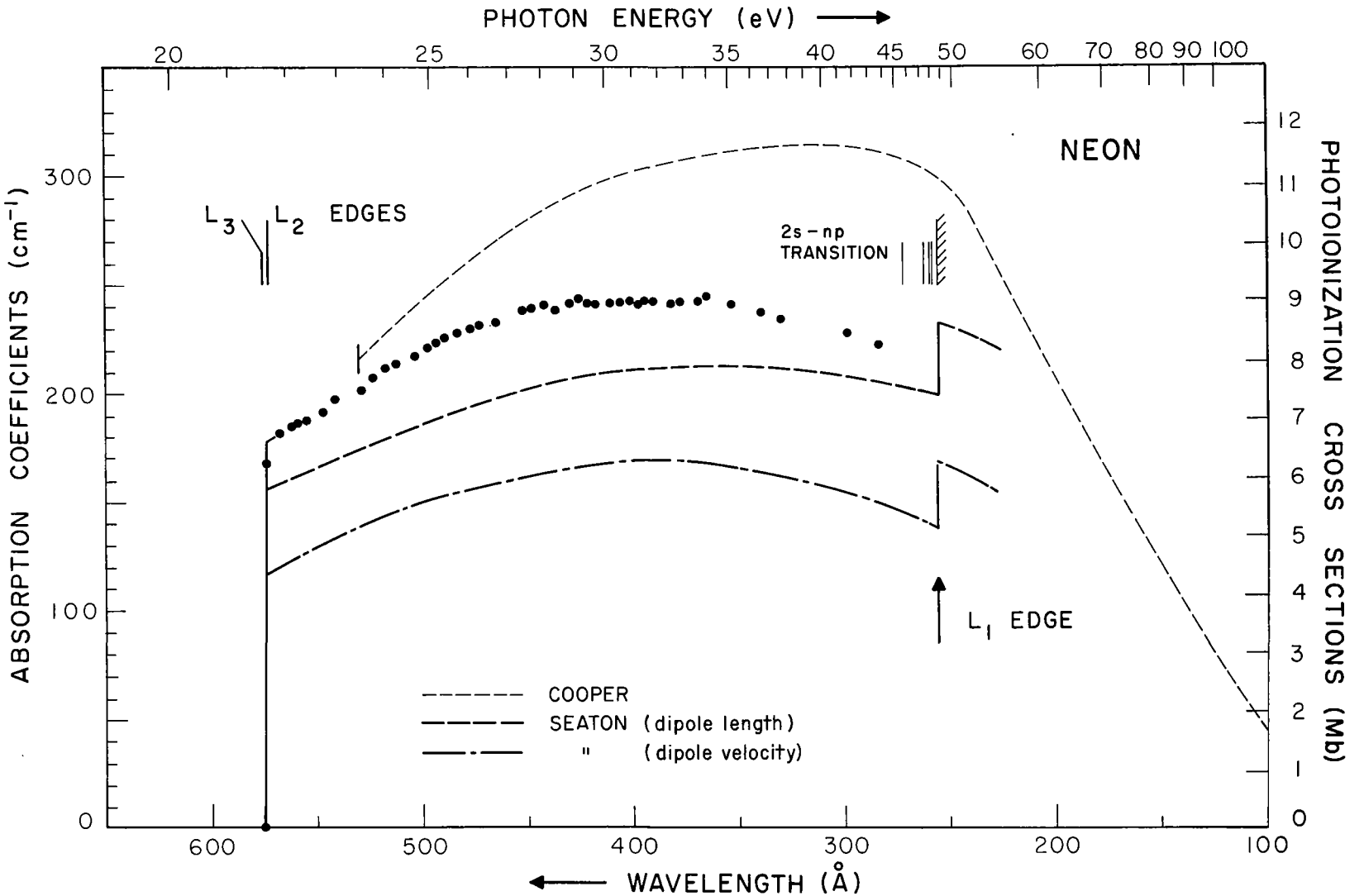

Figure 4. Photoionization cross sections of neon compared to theoretical values.

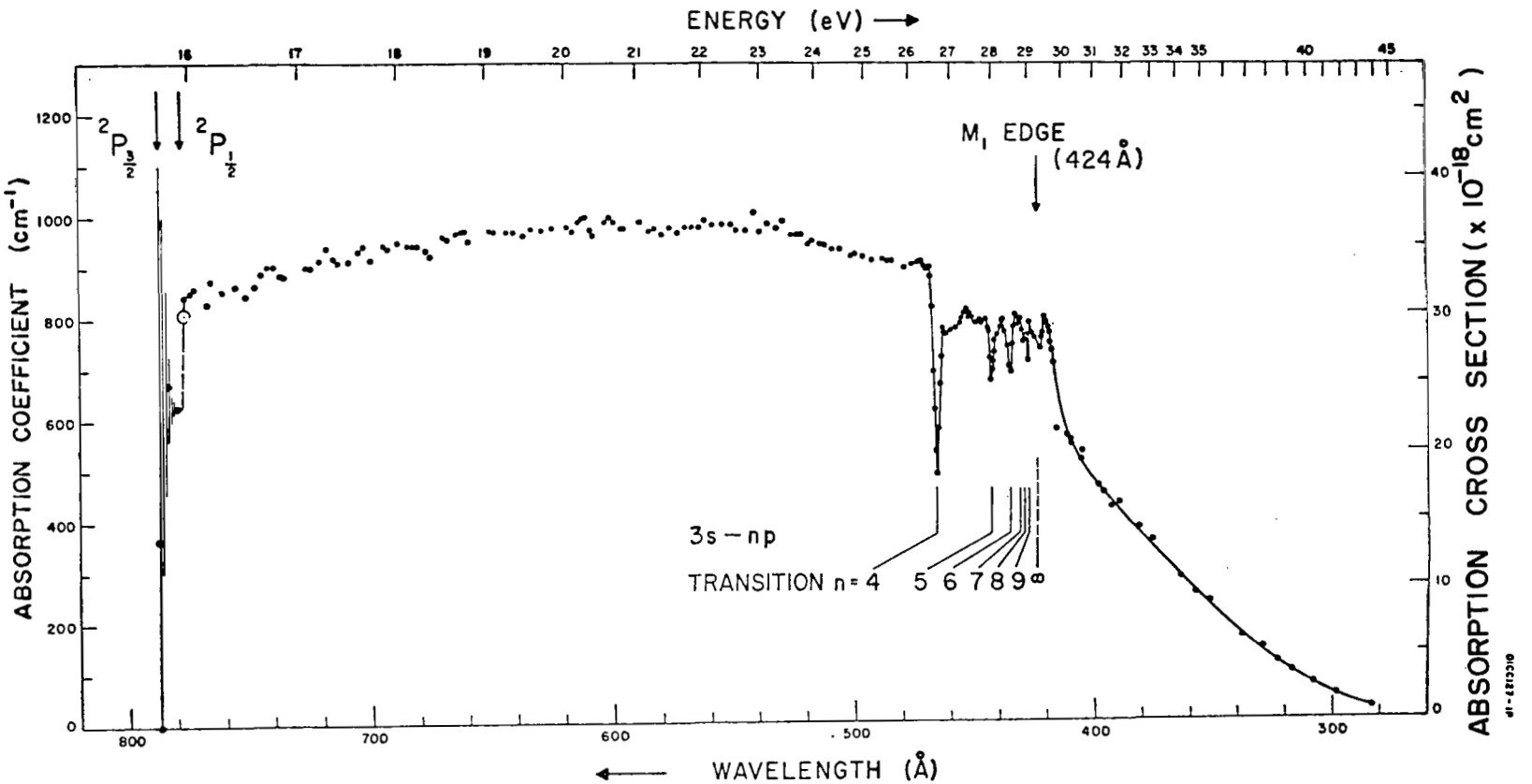

Figure 5. Photoionization cross sections of argon. The vertical lines between the $^2P_{3/2,1/2}$ edges indicate schematically the Beutler autoionization lines.

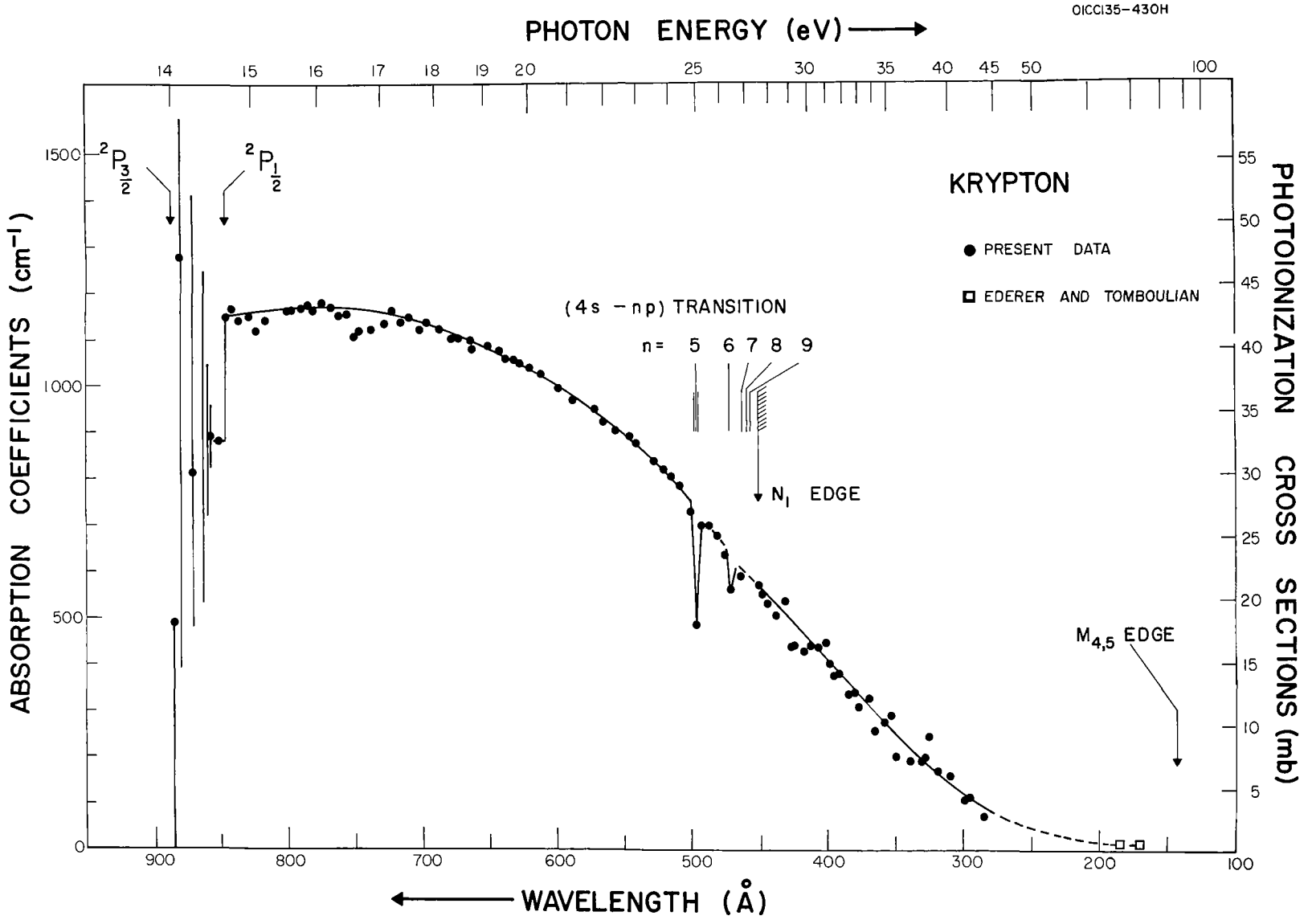

Figure 6. Photoionization cross sections of krypton. The vertical lines between the $^2P_{3/2,1/2}$ edges indicate schematically the Beutler autoionization lines.

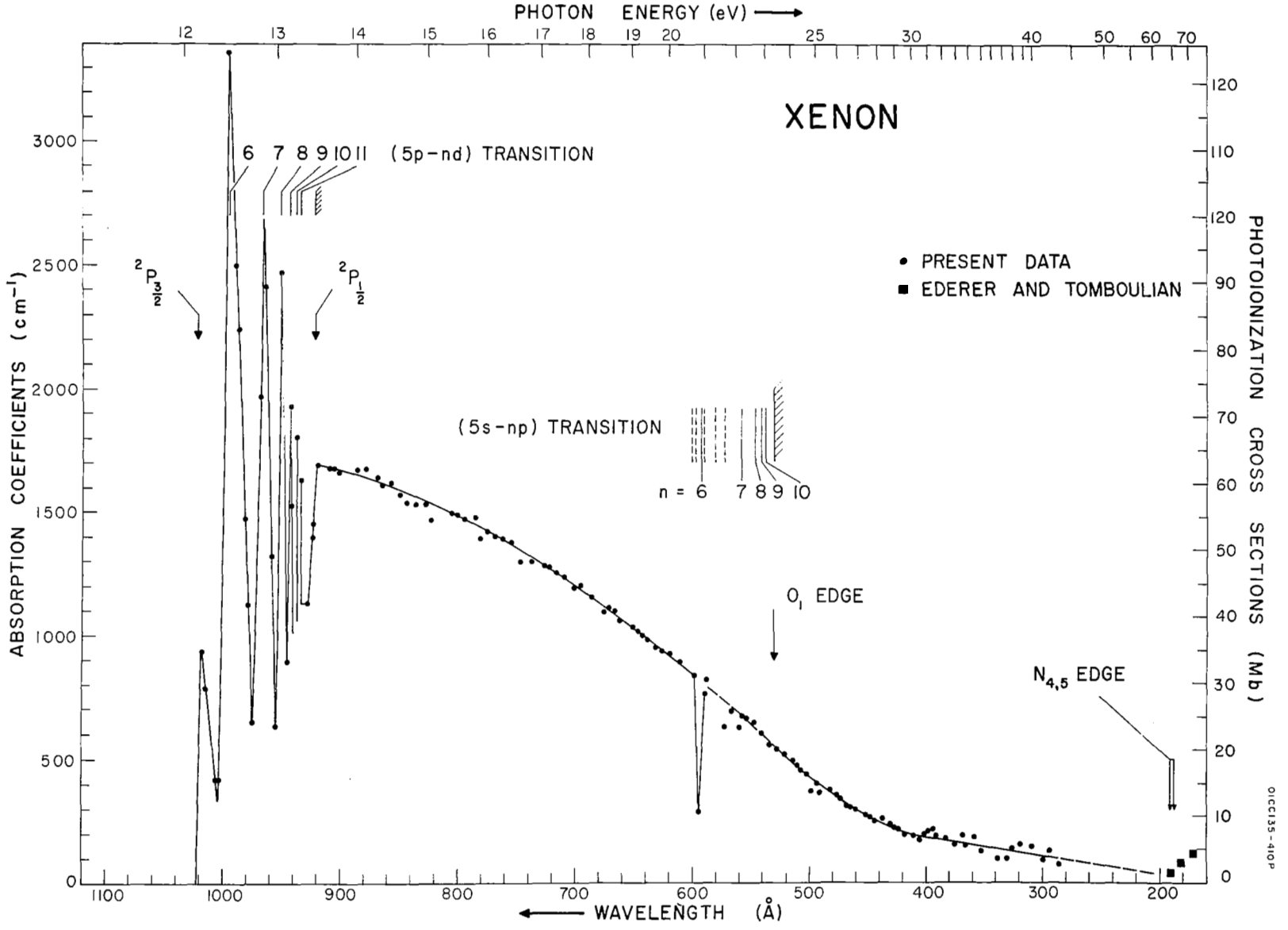

Figure 7. Photoionization cross sections of xenon. The data of Ederer and Tomboulian increase from the $N_{4,5}$ edge to a maximum of 30 Mb at 130Å.

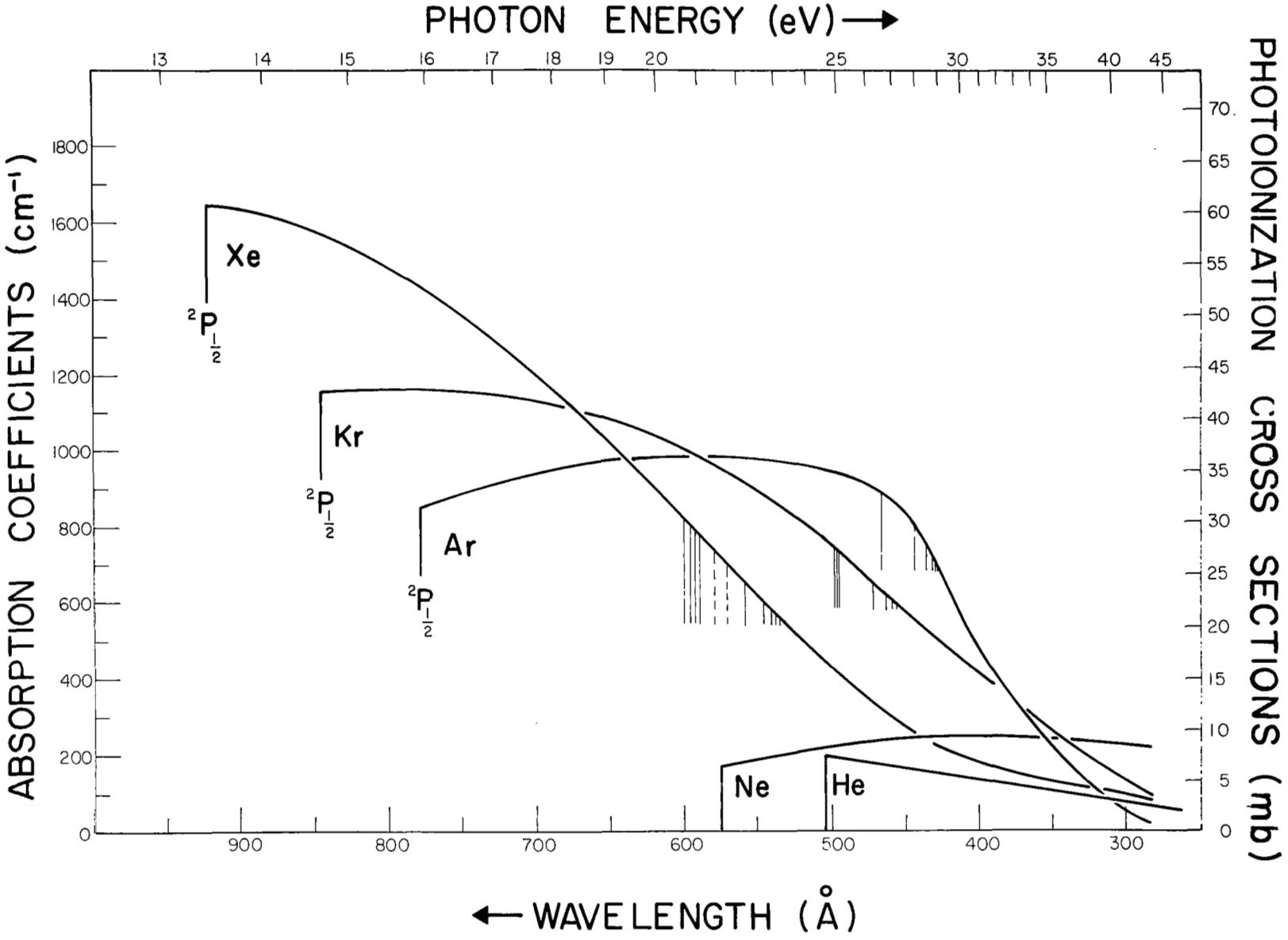

Figure 8. Absorption coefficient of He, Ne, Ar, Kr and Xe vs wavelength.

Nevertheless, they can be successfully used, although their application will be more specific. Figures 9 and 10 give the absorption characteristic of CO_2 and N_2O, respectively. A CO_2 filter, for instance, was used for the detection of acetone in butane at 1216Å. In order to increase the detection sensitivity for acetone in butane, it was again essential to have the filter cutoff as close as possible to the ionization onset of butane at 1170Å.

The absorption characteristic of N_2O is another typical example for the more complex behavior of molecular gases. It shows a bandpass at 1200Å and at 1400Å. Such a filter will be very well suited for the discrimination of two gases with ionization potentials of about 10.4 eV and < 9 eV, since the high absorption below 1200Å and between 1200 and 1400Å will result in a minimum of scattered wavelengths below 1400Å.

In certain cases it might be even possible to achieve discriminative ionization without a monochromator by use of uv filters which can combine different gases, thin films, and above 1000Å, certain solid materials like lithium fluoride or sapphire.

Light Sources

It is evident that the emission characteristics of the available uv light sources are also of great importance in connection with the question of short wavelength interference. Such interferences would be minimized if there were no light source emission below the wavelength required for the ionization of a certain gas. In principle, this can be achieved with a resonance uv light source; however, the limited number of available resonance lines as given in Table 1 does not permit much flexibility for discriminative ionization.

For a more general application, a continuum or at least a multi-line uv spectrum is the better choice, since it permits the selection of a wavelength close to the ionization threshold which often gives the highest ionization yield. Ideally, the spectrum should cover any wavelength in the total range of interest but show no emission at shorter wavelengths. The total range of interest, of course, depends strongly on the kind of gases or vapors to be analyzed. From 1700 to 780Å (7.3 to 16 eV), all known gases and vapors, except Ne and He, can be ionized selectively.

None of the known uv light sources which produce a multi-line spectrum or a continuum comes close to such ideal conditions and many compromises have to be made. The "rare gas continuum light source" does not give sufficient intensity for the application in an analytical photoionization mass spectrumeter; in addition, the continuum produced by one gas extends only over 200 to 300Å and the continue of the different rare gases do not adjoin without large gaps in between.

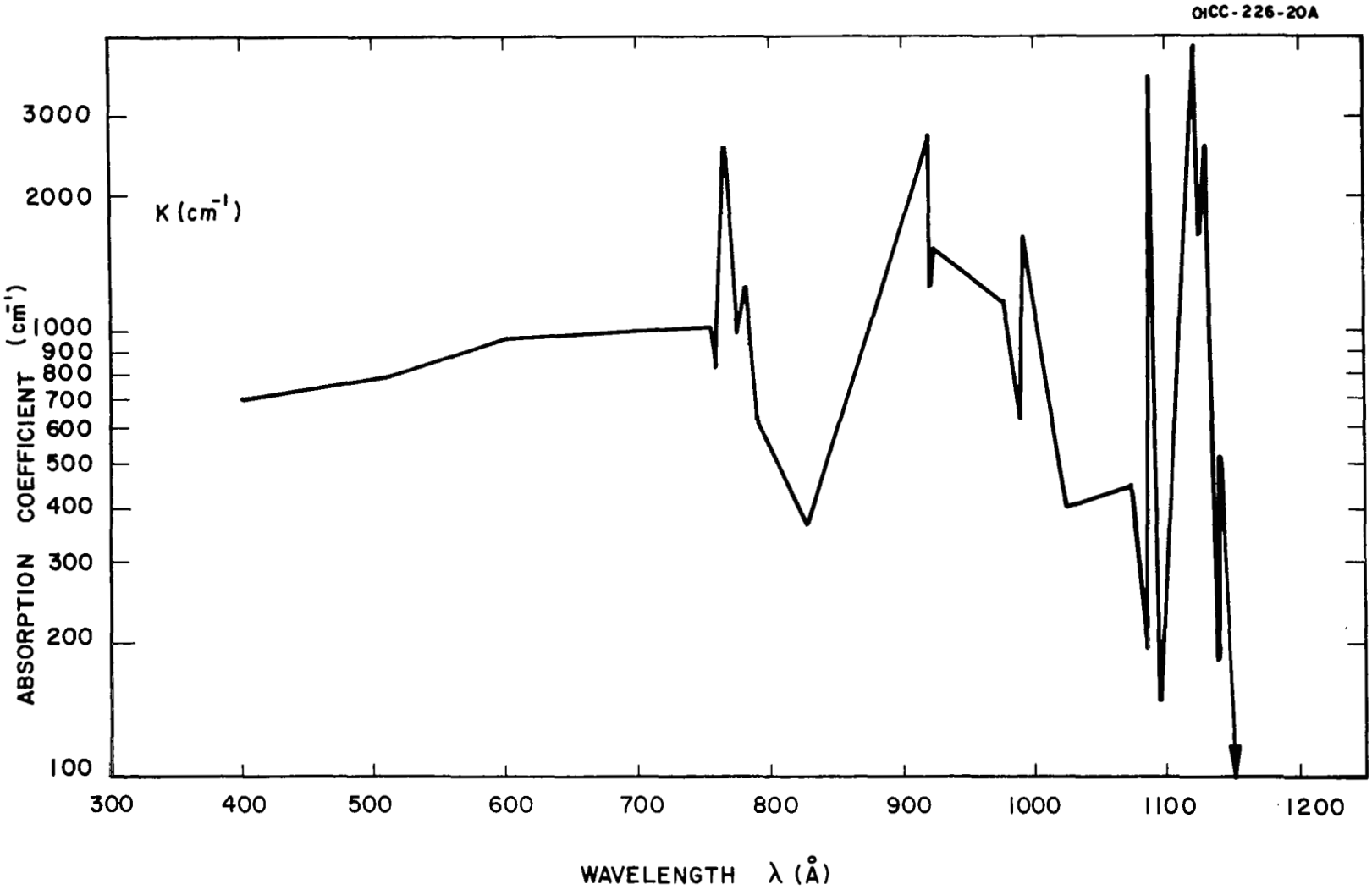

Figure 9. Absorption coefficient of CO_2

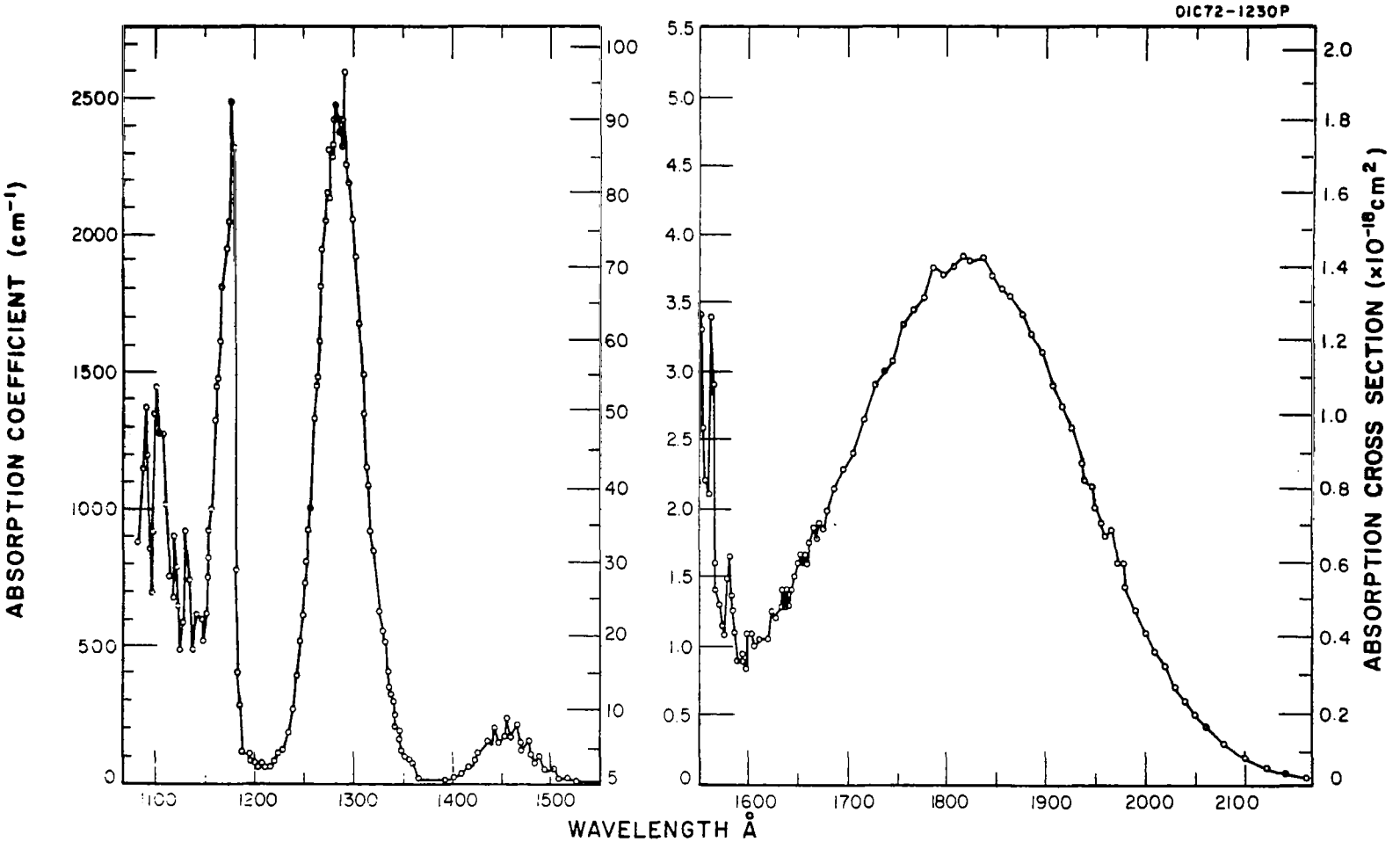

Figure 10. Absorption coefficients and cross sections of N_2O
λ = 1080Å to λ = 2160Å
Method: Photoelectric detection
Ref: K. Watanabe et al., AFCRC Tech. Rpt. No. 53-23, Geophys. Res. Paper No. 21 (1953).
Experimental error: 5 to 10 percent.

TABLE 1

RESONANCE LINES BETWEEN 500 AND 1500Å

Gas	λ (Å)	Gas	λ (Å)
Helium	584	Xenon	1295/1420
Neon	735/743	H	1216
Argon	1048/1066	Krypton	1165/1236

Sufficient intensity can be achieved with a pulsed spark light source; however, other disadvantages are encountered:

(a) The spark source delivers a line spectrum.

(b) Only very little intensity is emitted from 1000 to 1700Å; therefore, another light source has to be employed for this wavelength range of interest.

(c) On the other hand, the intense spark spectrum is not only emitted between 780 and 1000Å but also reaches down to about 400Å or even lower, depending on the gas used in the source.

The restriction under (a) is usually not too serious, since the spark spectrum comprises a great many intense lines and a certain flexibility can be achieved by using different gases or mixtures. The spark source spectra of N_2 and Ar are in Reference 1 and others can be found in Reference 5.

As mentioned under (b), the spark source cannot be used universally for the total range of interest, and above 1000Å, it has to be exchanged with an H_2 continuous discharge light source which delivers a multi-line spectrum of sufficient intensity at wavelengths larger than 1000Å. The typical H_2 spectrum is shown in Figure 11. The same type of source can also be used with rare gases to produce the resonance lines given in Table 1. More detailed data can be found in the literature [5,6].

The emission of an intense spectrum below 780Å, as mentioned under (c), necessitates the use of filters. A study of the pressure dependence of the spark spectrum revealed, however, that under certain conditions, a strong suppression of the emission below 780Å can be obtained in the spark source itself. The situation is particularly favorable if the spark source is run with Ar. This is demonstrated in Figure 12. At an Ar pressure of 25μ in the light source, one obtains the typical low pressure spark spectrum of Ar which extends well below 780Å and down to about 400Å (see also Figure 12 in Reference 1). At 50μ, a drop of the intensity below 780Å is observed which becomes even more significant at 100μ. At 200μ, no emission below 780Å can be detected with the used sensitivity. This effect is obviously caused by self-absorption in the light source itself. The amount of neutral gas, which increases with the pressure, acts like a gas filter within the source. In addition, some changes in excitation conditions as function of pressure is observed in relative line intensity variations; e.g., at 25μ, the 835Å line is dominant while at 200μ, the 879Å line is more intense. It should be mentioned, however, that these excitation conditions also depend on discharge current and pulse shape. Fortunately, the Ar spark spectrum at 200μ pressure also has a comparatively dense line structure between 780 and 1000Å which altogether makes it superior to the spark spectra of other gases. (The strong intensity of the 879Å line at 200μ was particularly favorable for the detection of CO because of the high photoionization yield of CO at this wavelength.)

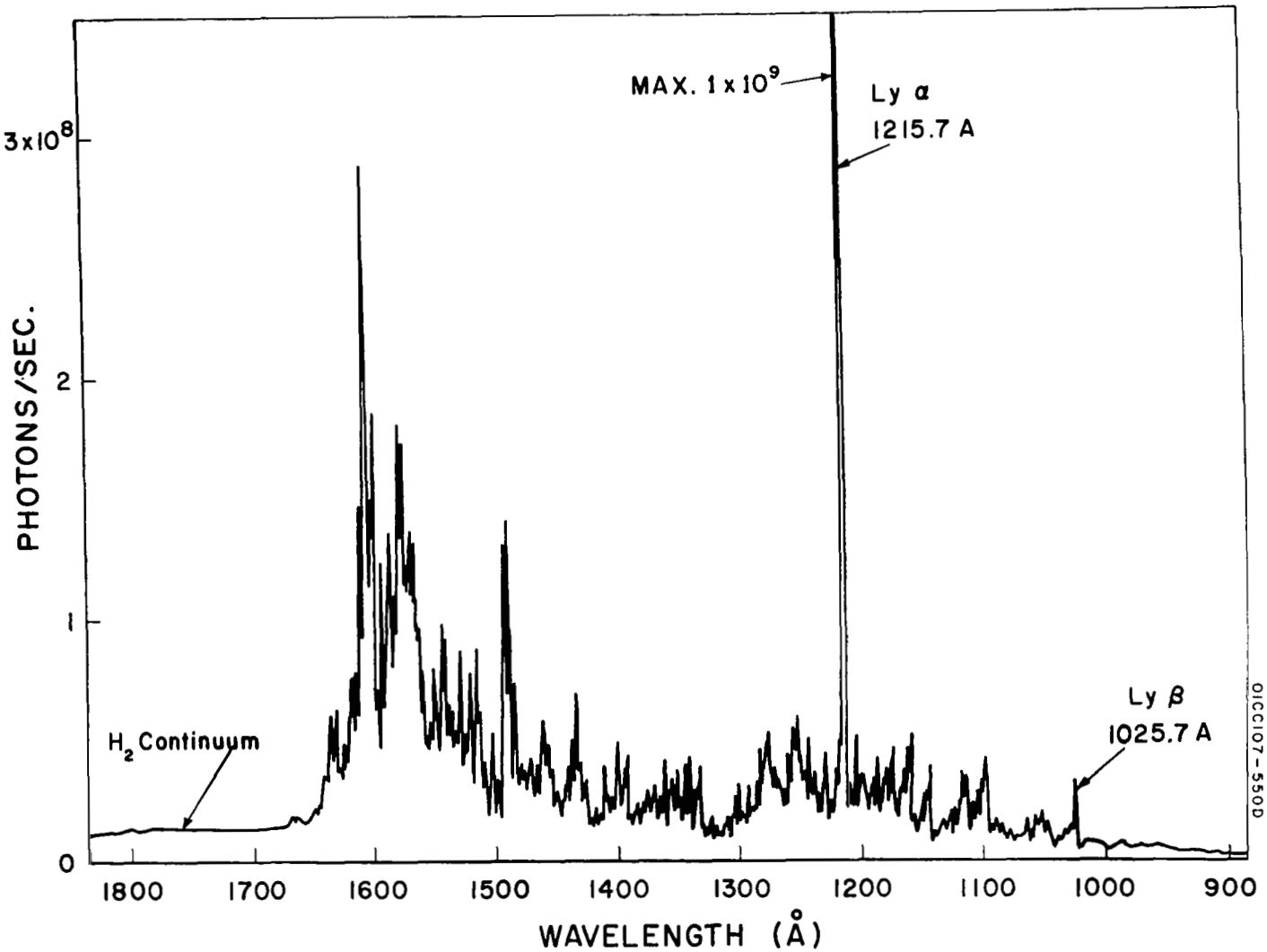

Figure 11. Hydrogen spectrum taken with an arc current of 0.9 amp. Wavelength resolution is approximately 2 Angstroms.

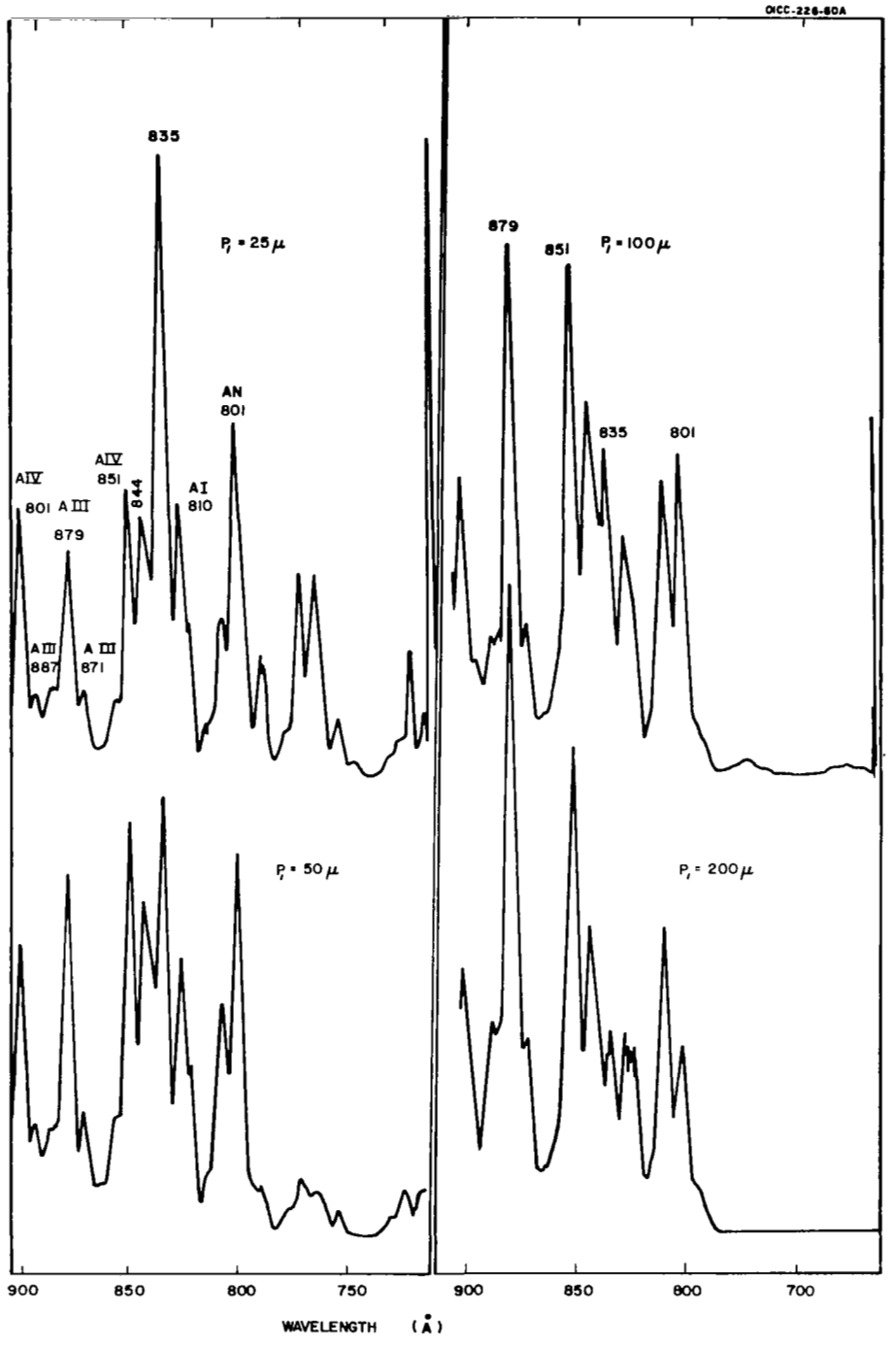

Figure 12. Pressure dependence of Ar spark source spectrum.

THE NEW MONOCHROMATOR

During the initial experiments under Contract No. NASI-4927, the photoionization mass spectrometer was combined with a McPherson 1/2-meter Seya monochromator. The incorporation of a thin-metal filter and the gas filter into this instrument would have been difficult because of its cast iron housing. The McPherson monochromator was not a deliverable part under the final contract. It was supplied by GCA for the experiments. Since the present contract includes delivery of a monochromator, it was decided to use a monochromator system developed and constructed by GCA instead of purchasing another commercial instrument. The GCA monochromator is constructed from stainless steel, which makes the necessary modifications and the adaption to the photoionization mass spectrometer much easier.

The GCA 1/2-meter Seya monochromator is a vacuum monochromator designed for use throughout the spectral range from 8200 to 200Å. Particular consideration has been given to the performance of this instrument at wavelengths shorter than 1500Å, where lithium fluoride optics can no longer be employed.

The Seya monochromator is a tabletop model constructed from 304 stainless steel in such a manner that it can be easily disassembled and cleaned. It has a rotatable grating mounted on a solid stainless steel base 1/2-inch thick. The system is evacuated through an opening in the base. A cylindrical vacuum housing 10 inches in diameter and 8-1/2 inches high, flanged at top and bottom, mounts onto this base. This cylinder has two arms (3 in. long) set such that their axes subtend an angle of 70 degrees 30 minutes at the center of the grating. These short arms are flanged to accept extension tubes of any desired lengths. This feature permits a rapid and economical conversion from a 1/2-meter to a 1- or 2-meter monochromator with corresponding improvements in wavelength resolution (of course, the appropriate gratings have to be used). The f-number of the 1/2-meter version is about 10. A high precision sine-drive screw used in the wavelength scanning mechanism provides wavelength identification with an accuracy of about 0.1Å. Ten scanning speeds are available within the range from 2000 to 2Å per minute. The scanning control has between each speed a neutral position at which the grating can be rotated manually. The instrument can be scanned over a wavelength range from 0 to 8200Å with a 600 lines/min grating.

The extension tubes which come with the standard monochromator, and the usual exit and entrance slit portion were replaced by arms specially made for the adaptation to the photoionization mass spectrometer. The entrance arm contains the entrance slit and part of the gas filter. A gate valve directly behind the entrance slit permits the isolation of the light source from the monochromator; thus, exchange of the light source is possible without venting the monochromator. Further provisions are made to accommodate the thin-film filter unit directly in front of the entrance slit. The chamber between light source and entrance slit can be pumped differentially. The

outer flange has an outside diameter of 5 in., an 'O' ring groove with an inside diameter of 3-3/4 in. and a 3-hole half-circle with 4-1/2 in. diameter. Consequently, all GCA light sources and most of those from other manufacturers will match. Since the exit slit is an integrated part of the ion source, the exit extension arm is a plain tube and the adaptation piece of the mass spectrometer slides into it much the sameway as previously into the exit arm of the McPherson monochromator.

The monochromator is equipped with a Bausch and Lomb replica grating ruled with 1200 lines/min and a blaze angle of 1500Å. The grating is gold plated to provide high reflectivity in the uv range.

The monochromator is mounted on a sturdy table which matches the mass spectrometer table. It is supported on a frame with adjustment screws which allow precise height adjustment and levelling.

A CVC PMC720 4 in. diffusion pump and a multicoolant baffle evacuate the monochromator and provide a pump speed of about 300 ℓ/sec. The monochromator table also provides space for the two Welch 1397B forepumps which supply the forevacuum for the entire system.

Figure 13 shows the new monochromator attached to the mass spectrometer and ready for the first preliminary tests.

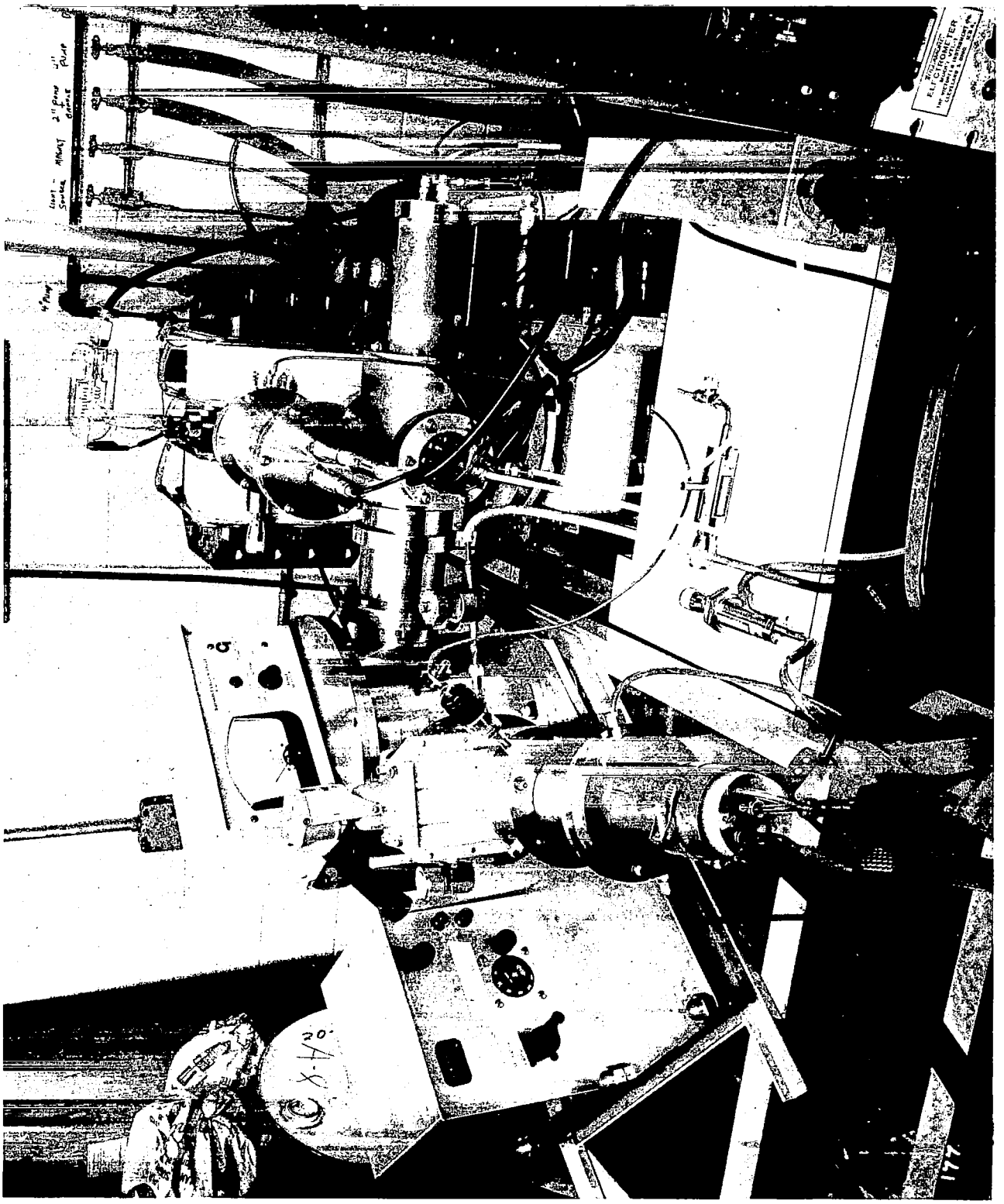

Figure 13.

DESIGN AND CONSTRUCTION OF THE FILTER UNITS

The Thin-Film Filter

It has already been stated that of all thin-metal filters, only an indium film provides a suitable filter characteristic for use in the photoionization mass spectrometer. The thickness of such an indium film must not exceed 3000 to 4000Å or the transmission in the range of transmittance becomes less than 10 percent. It is evident that the fabrication of such thin films requires some special care.

First, a thin film of indium is evaporated onto a water soluble substrate (Victawet) which has been sprayed onto a slice of glass. High vacuum and cleanliness are the necessary preconditions for a good film, since the presence of foreign bodies will cause irregularities and pinholes in the film. When the glass slice with the indium film on top is slowly immerged, the substrate is dissolved and the film of indium is brought to float on the surface. Finally, the film is lifted off with a piece of high transmission mesh which further serves as a mechanical support for the very delicate film.

After the successful fabrication of such a thin film, measures have to be taken for its protection. The film is easily damaged by even small pressure differentials as may occur when the monochromator is vented. It is also useful to have an arrangement which switches the filter into the light path or pulls it out as needed. A simple magnetically activated device was therefore constructed which either moves the filter into the light beam or retracts it into a protecting sheath. Figure 14 shows the construction of this unit.

The mesh which supports the indium film is mounted on a stainless steel ring. As soon as the solenoid is activated, this ring will be pulled into the center of the disc through which the light beam passes. The filter slides immediately back into its protective space when the solenoid current is interrupted.

The Gas Filter Cell

In the design of the gas filter, a number of problems were encountered. The absorption cross sections of the various gases shown in Figures 3 to 10 lie between 1 and 5 x $10^{-17}/cm^2$. The total absorption in the gas filter is obtained by Lambert-Beer's law:

$$I = I_o \exp(-n\sigma L) \qquad (1)$$

where I_o is the photon flux incident upon the absorbing gas; I is the transmitted flux; L is the length of the absorbing path; and n is the number density (per cm^3) of the absorbing gas. The number density at 1μ pressure is 3.5 x $10^{13}/cm^3$. The length of the gas filter is mainly limited by the geometry of the light path and lies between 10 and 30 cm. For a reduction of the incident light by a factor of 100, Equation (1) yields:

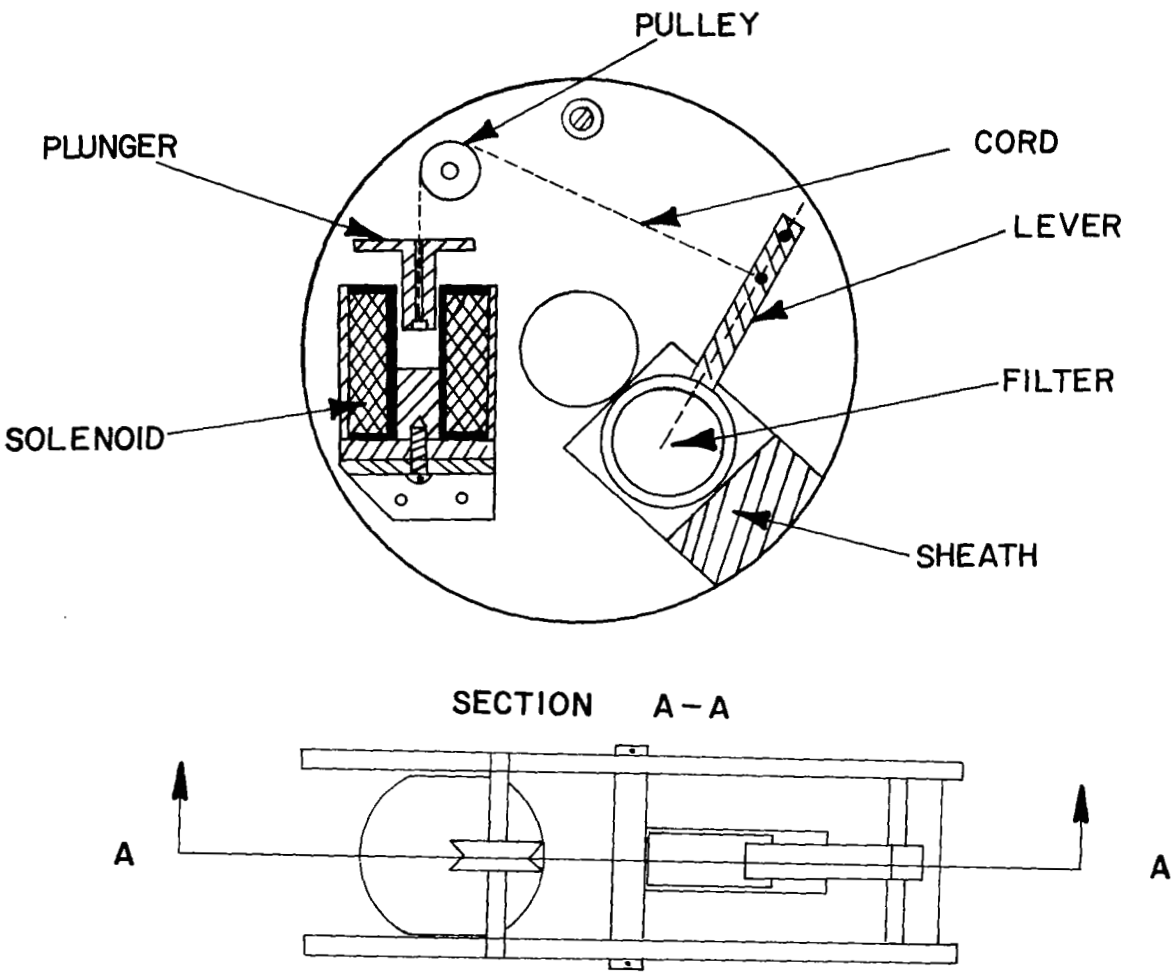

Figure 14. Thin film filter assembly.

$$n\sigma L = 4.6 \qquad (2)$$

It follows that the gas pressure in the cell has to be between 0.09 and 1.4 torr for the considered range of L and σ.

No solid windows are known which can be used below 1040A to seal the ends of the filter cell; therefore, a considerable amount of gas will also flow through the openings through which the light beam enters and leaves. Obviously, one has to compromise on the size of these openings in such a way that the flow of gas can still be handled by the vacuum system, while the aperture of the light beam is not too drastically reduced. The question was: can a reasonable compromise be achieved within practical and economical limitations? The first decision conerns the location of the filter. One condition for a good placement is fulfilled when the aperture of the light beam is least affected; a second requirement is that the filter does not cause any other interference.

The first condition can be best satisfied if the filter cell is directly adjoined to either the entrance or exit slit. In this case, the slit itself represents one opening, while the other opening determines the aperture of the light beam in the monochromator. Further considerations immediately exclude any placement of the gas filter on either side of the exit slit, because of the construction of the ion source and the danger of glow discharges in this region with high electric potentials. The proximity of the filter to the ion source would also cause a considerable flow of filter gas into the ion source and, therefore, obscure the spectrum of the sample gas. The remaining choice is now to put the filter between either light source and entrance slit or entrance slit and grating.

The design of the McPherson monochromator would have made it difficult to place the gas filter between entrance slit and grating. Consequently, it was originally suggested that the gas filter be located between light source and entrance slit. In this arrangement, the light source has to be moved away from the entrance slit by the length of the filter cell. This has one distinct disadvantage: the diameter of the spark discharge is only a few mm and the usable aperture of the monochromator is not fully utilized. This leads to a loss in intensity which increases with the distance between light source and entrance slit. If one kept this distance short, an exceedingly high pressure would be required to achieve sufficient absorption. This high pressure would cause a serious problem, particularly if the light source is run with a gas different from the filter gas.

The use of the GCA monochromator makes it possible to consider the integration of the gas filter directly into the monochromator between entrance slit and grating. Also in this case, a reasonable filter performance, with a minimum of loss in intensity by aperture limitation, must be compatible with the vacuum requirements.

If the entrance slit of the monochromator forms one end of the filter cell, then the aperture of the light beam is given by the diameter D of the filter cell exit opening and the distance L between both. For the following, one may neglect the width and height of the entrance slit and also that the Seya-type monochromator does not give a fully stigmatic image. The total photon flux I through the monochromator is then proportional to the effective solid angle of the light beam, and we may write:

$$I = C_1 \left(\frac{D}{L} \right)^2 , \quad C_1 = \text{const.} \tag{3}$$

As shown by Equations (1) and (2), the product nxL is determined by the requirement of sufficient absorption. Since n is proportional to the cell pressure p_c, Equation (2) can be written as

$$p_c . L = C_2 \tag{4}$$

The question now is: can a minimum of gas flow into the monochromator be achieved for a certain fixed value of I and $p_c.L$ by changing L? The flow of gas out of the filter cell is a function of D and p. This function cannot be described by a simple equation because the flow in the considered range of D and p lies in the transition region between Poisseulle and jet flow. Nevertheless, sufficient information can be gained when the results for both flows are compared. If Q_m is the maximum flow which can be tolerated, we obtain for Poisseulle's flow:

$$D^4 . p_c^{\,2} \, C_p = Q_m , \quad C_p = \text{const.} \tag{5a}$$

and for the jet flow:

$$D^2 . p_c . C_j = Q_m , \quad C_j = \text{const.} \tag{5b}$$

The pressure in the monochromator has to be more than one order of magnitude below p_c and can be neglected in Equations (5a) and (5b).

Combining Equations (3), (4) and (5a), we obtain:

$$I = \frac{1}{L} \frac{C_1}{C_2} \sqrt{\frac{Q_m}{C_p}} \tag{6a}$$

and Equations (3), (4) and (5b):

$$I = \frac{1}{L} \frac{C_1}{C_2 C_j} Q_m \tag{6b}$$

In both cases, the aperture determined intensity I is inversely proportional to the length L of the filter cell. Obviously, a shorter cell with a higher pressure, according to Equation (4), represents the better solution; however, if the pressure becomes higher, the flow through the entrance slit into the light source region must be considered. Obviously, one will have to look for a compromise. Comparing Equations (6a) and (6b), one also finds that the selection of the proper dimension is more critical under the Poisseulle flow condition since the flow Q increases with L^2 if I is held constant and is not just proportional to L as in the jet flow range. The inverse relationship between I and L also holds true for the transition range, but the dependence of the flow Q of L will be a more complex function in between L and L^2.

The foregoing considerations give sufficient information for a practical design in spite of all generalizations and approximations. In the following, three different practical solutions are discussed. For these practical layouts, it was decided to keep the cell pressure between 100 and 500μ and the length at 25 cm, which matches the requirements expressed in Equation (2) reasonably well. In addition, an aperture of the light beam which uses about 3/4-in. of the total 2-in. grating was deemed to be sufficient, since the present spark source by its geometry does not illuminate a solid angle much larger than this. The distance between entrance slit and grating is about 40 cm; therefore, the light beam should leave the filter through a 10 to 11 mm diameter opening.

Solution 1: The filter cell is 25 cm long with an entrance slit on one side and an opening hole 1 cm in diameter and 1 cm long on the other end; diameter of the cell is large compared with openings to achieve about equal pressure within the cell volume. The layout is sketched in Figure 15. Tables for the calculation of the actual flow were given by Diels and Jaeckel [7]. For the conditions suggested above and a pressure of 100μ, a flow of 0.5 torr-liters/sec is obtained. For p = 500μ, the flow increases to 4.5 torrliters/sec.

Solution 2: The cell is again 25 cm long but has a diameter of 1 cm over its entire length (Figure 15). In this case, the flow resistance is approximately evenly distributed over the total length of the cell and the pressure drops about linearly with the distance from the gas inlet, which should be close to the entrance slit. The number n of absorbing atoms in Equation (2) is obtained by taking the average pressure in the cell, which is simply half the pressure at the gas inlet. For an average pressure of 100μ, a flow of 0.15 torrliters/sec is obtained and for 500μ, 3 torrliters/sec, respectively.

Solution 3: The principal arrangement, as shown in Figure 15, is similar to Solution 1, but an additional buffer chamber is put between the cell and the monochromator. The filter cell is now 20 cm long and the buffer chamber 5 cm. The openings are chosen so as to permit the same aperture of the light beam as before, and the buffer chamber has provisions for differential pumping. If K_1 is the conductivity of the opening between gas cell and buffer chamber, K_2 the conductivity of the hole between buffer chamber and monochromator, p_c the cell pressure, p_o the pressure in the buffer chamber, and S the pump speed available for differential pumping, one can write:

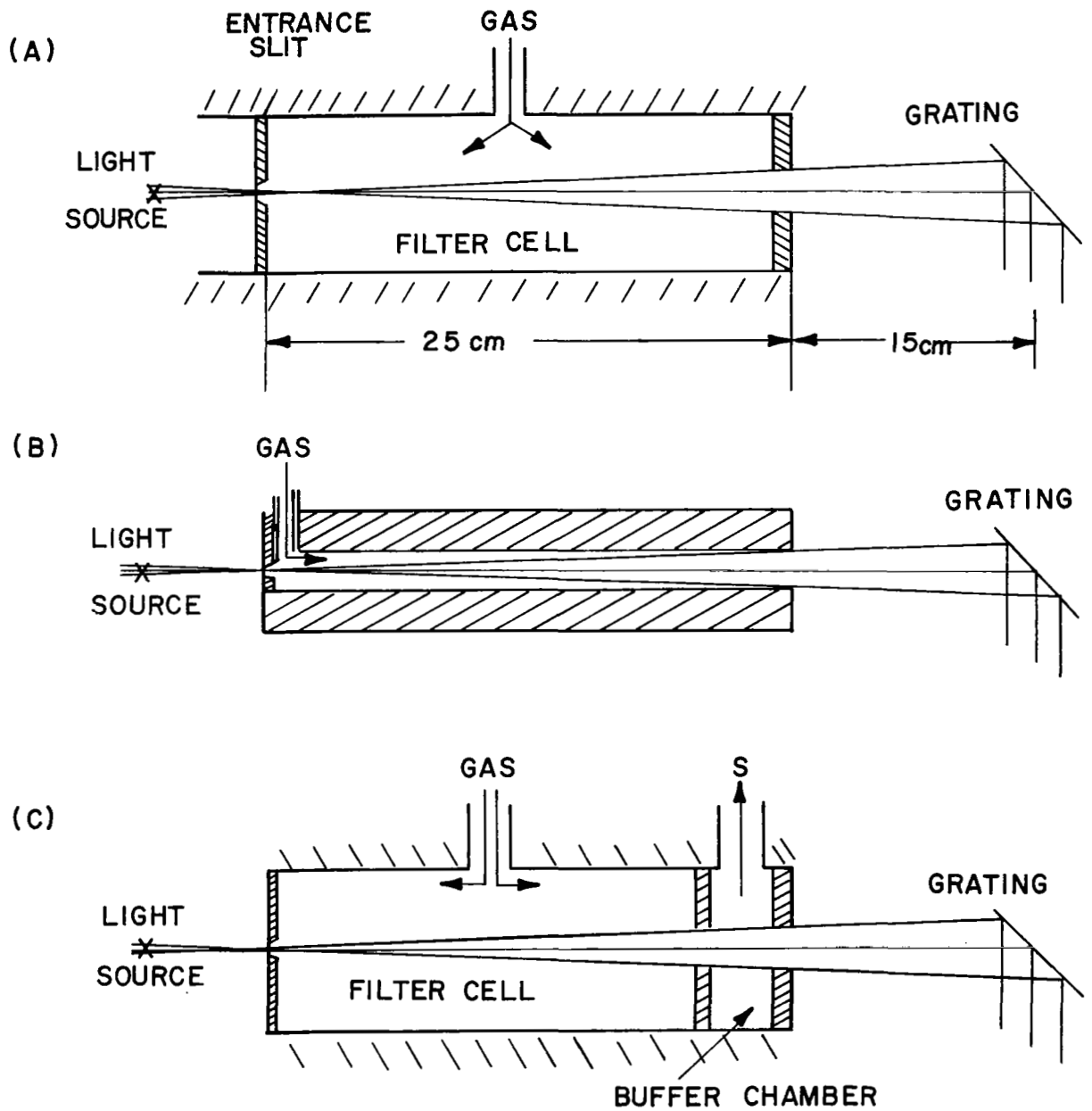

Figure 15. Different gas filter geometries

$$p_o = p_c \frac{K_1}{K_1 + K_2 + S} \qquad (7)$$

For a pressure p_c of 500μ, K_1 and K_2 are approximately 7 ℓ/sec. A pump speed S = 7 ℓ/sec can be obtained with one forepump 1390B; therefore, Equation (7) yields

$$p_o = \frac{500}{3} = 166 \text{ torr}$$

Without differential pumping, S = 0 and Equation (7) then gives:

$$p_o = \frac{500}{2} = 250 \text{ torr}$$

One can see that differential pumping gives only a slight improvement because of the practical limitations in pump speed. It is now necessary to evaluate the different solutions in connection with the existing vacuum system.

The monochromator is pumped by a CVC PMC 720 with a multicoolant baffle. The total photoionization mass spectrometer is backed by two Welch 1390B forepumps, but since the gas load from the mass spectrometer is small, most of the pump speed may be utilized for the monochromator including gas filter and light source. The graphic evaluation shown in Figure 16 is based on data given by the manufacturers. One sees that Solution 1 would only permit a cell pressure of 300μ if the diffusion pump were backed by one 1390B forepump. Two forepumps in parallel will just match the maximum throughput of the PMC 720 with baffle; and under these conditions, Solution 1 permits a pressure of 400μ. Solution 2 gives 400 and 550μ with one or two forepumps, respectively. Solution 3a (without differential pumping) will just permit the required pressure of 500μ with one forepump alone. Since two forepumps are available, one can either select Solution 3b with differential pumping or Solution 3a with two pumps in parallel. Figure 16 shows that the limiting pressure is about 700μ for either case. Quite different, however, is the pressure in the monochromator which is 6 or 30μ, respectively.

The final choice was made in favor of Solution 3a but with provisions for differential pumping if needed. Solution 2, which could also have been improved by the addition of the buffer chamber, was finally rejected because it was feared that the long narrow tube could cause considerable light scattering. On the other hand, Solution 3a with one forepump seems to be quite sufficient, particularly since the availability of the second forepump, either pumping parallel to the other pump or differentially alone, offers sufficient reserve in case the calculation was not precise. Differential pumping could also be employed if it turned out that a pressure of 5 to 10μ in the monochromator would cause a problem.

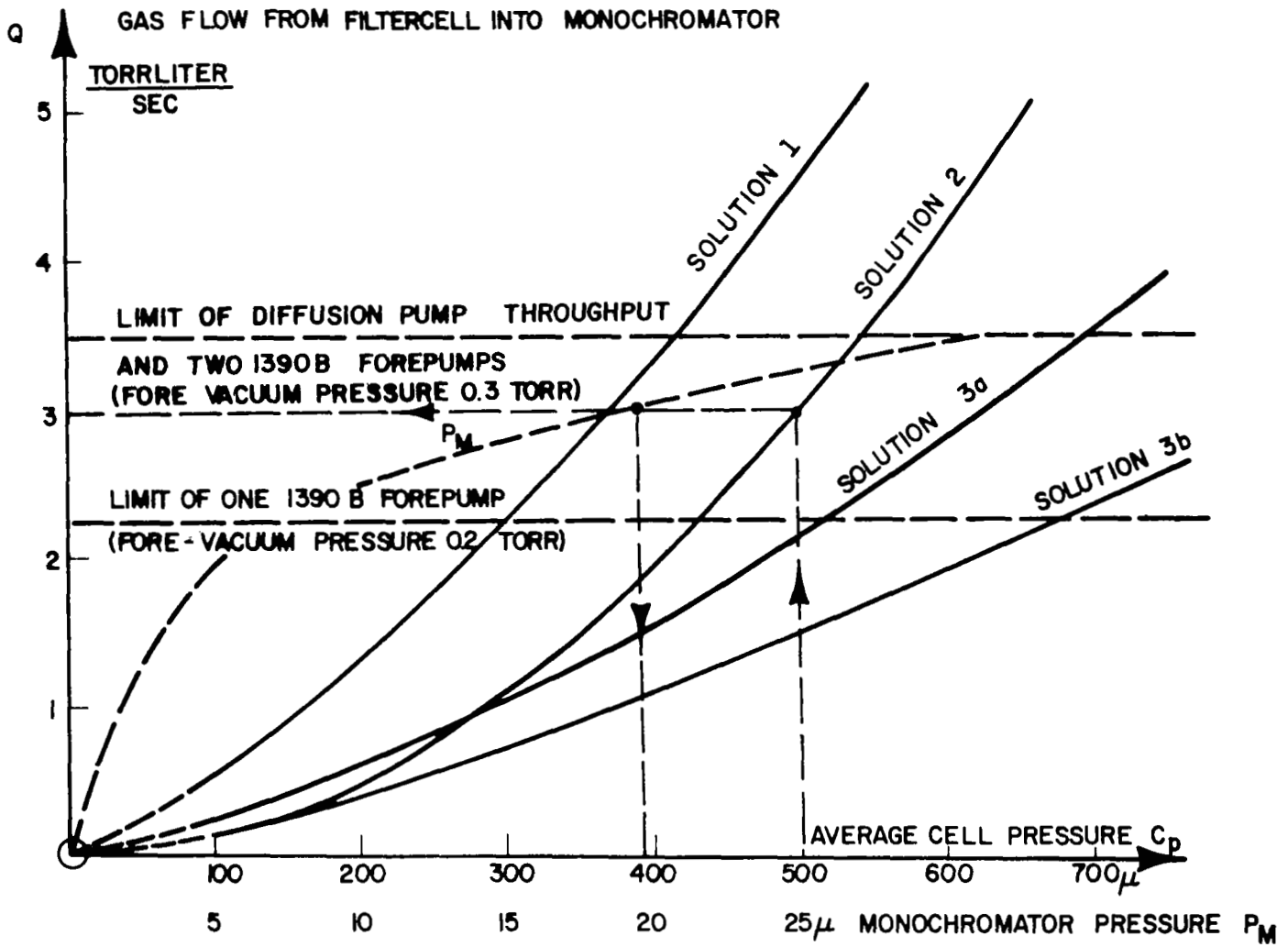

Figure 16. Flow diagram for different gas filter designs.

The experimental tests of the gas filter have shown a good agreement with the calculated performance. The construction of the actual gas filter is very simple. The buffer chamber is contained in the short part of the entrance arm which is welded into the large grating housing cylinder. It consists of two discs sealed against the tube walls with an O-ring and located at both ends of the short arm. The disc toward the grating has an 11 mm dia. center hole; the disc toward the entrance slit has a 9.5 mm dia. hole. Both discs are 12.5 mm thick and spaced 5 cm apart. A knife-edged aperture plate with a 10 cm diamter and an 8 mm diameter opening, respectively, is put in front of the disc holes to prevent scattering of light from the walls of the holes. All parts close to the light beam are blackened with soot. A 1 inch I.D. pump connection provides for differential pumping between both discs. The gas cell itself is formed by the entire section of the arm between buffer chamber and entrance slit. A micrometer valve on 1/4-inch inlet pipe regulates the gas pressure in the cell, and the pressure is measured with a thermocouple Hasting gauge.

THE IMPROVED ELECTRON DEFLECTOR

During the first tests of the new arrangement, employing an Ar gas filter, an unexpectedly high residual ionization of N_2 was observed at wavelengths above the ionization wavelength. This was in contradiction to the result obtained from the photomultiplier. That result clearly showed that the intensity of the spectrum below 780Å was at least reduced by a factor of 100. Consecutive investigations revealed electrons as the source of this background ionization. The electrons were produced within the monochromator and accelerated into the ion source which is on a high positive potential. A certain structure observed in this background spectrum when the monochromator was scanned indicated that most of these electrons were produced by the strong central image of the grating. This effect had already been suspected during the development contract of the photoionization mass spectrometer and an electron deflector had been incorporated between monochromator and ion source. This electron deflector obviously was not efficient enough to cope with the improvement achieved by the introduction of the filter. Previously, this problem had been obscured by the interferences of shorter wavelengths, but now the higher pressure in the monochromator, caused by the use of the gas filter, emphasized this effect since higher pressure leads to a higher electron production. Consequently, the electron deflector was improved and a reduction in the background signal of at least one order of magnitude was observed.

The new electron deflector consists of a pair of deflection plates which produce a field perpendicular to the light beam. The deflector is 4 cm long and mounted into the diaphragm insert between monochromator and ion source. One plate is on the same potential as the diaphragm aperture disc, which is about 100 volts more positive than the ion source; the other plate is on ground potential. With the new geometry, no electron can possibly pass from the monochromator into the ion source.

EXPERIMENTAL

Test of the Grating

Under Contract No. NAS1-4927, a 1200 lines/mm platinum-coated grating blazed for 750Å had been used. For this contract, it was decided to use a 1200 lines/mm gold-coated grating with a blaze of 1500Å for the following reasons:

In addition to the mentioned filtering methods, one can reduce the contribution of the short wavelengths to the principal ionizing radiation by a choice of the material used to coat the monochromator grating. Since reflectivity varies with wavelength, one can, in principle, select a coating which shows poor reflectance in the short wavelength region but good reflectance in the spectral region of main interest. For normal incidence, the reflectivity generally declines with decreasing wavelength, but this effect is enhanced for some materials. By comparison of reflectance data for various metallic coatings, it was found that gold gives a better discrimination against shorter wavelengths than the platinum coating used before. In addition, gold coating is less prone to form blisters on the grating which cause scattering of light.

The performance of the present gold-coated grating was compared with the earlier used platinum-coated grating. It was found that the light intensities received at the photomultiplier under otherwise identical conditions were about equal for the two gratings at 548Å, about twice for the platinized grating at 880Å, and about four times greater at 1216Å. A somewhat lower yield of the gold-coated grating at the longer wavelengths was expected in view of the lower reflectivity of gold, but the equivalence of the intensity at 584Å did not conform to the available reflectance data. It is possible, however, that the reflectance of the platinum-coated grating has decreased with use, whereas the gold-coated grating was new. Indeed, the platinized grating showed some surface roughness presumably caused by sputtering from the spark light source. Further tests revealed that the intensity of the second order He 584Å line was about 30 percent lower when the gold-coated grating was used. This is no advantage, since in the wavelength region of 1168Å, where the second order 584Å line appears, the first order intensity of the gold grating is worse by a factor of four than that of the platinized grating. For a full evaluation of this comparative test, it has to be taken into account that both gratings also have different blaze angles. The platinum-coated grating is blazed for a wavelength of 750Å, which enhances the intensity of the spectrum around 750Å. This is also true for all parts of the higher order spectra which are dispersed in the same direction of the first order at 750Å. The gold-coated grating was blazed for 1500Å.

The performance of the gold-coated grating between 800 and 1200Å was somewhat disappointing since the loss in intensity was more than was expected. In the light of the excellent performance of the gas filter, the stated advantage of the gold-coated grating and of a blaze for a higher wavelength becomes immaterial in contrast to the accompanying loss in intensity. Therefore, it is suggested for the future to go back to a platinized grating blazed for 750Å.

Separation of Doublets by Ionization Wavelength Discrimination

Utilization of the Gas Filter. Figure 17 demonstrates the effectiveness of the gas filter with Ar as filter gas. In this case, the Ar spark source was run at low pressure to prevent any suppression of emission below 800Å already in the light source. The unfiltered spectrum is given in the upper trace. A pressure of 500μ of argon in the gas filter was used for the lower trace. The sharp cutoff below 790Å is quite impressive. Increased detection sensitivity in the cutoff range indicates a suppression of the uv radiation by at least two orders of magnitude.

CO-N_2. The ability to separate CO and N_2 at M = 28 was taken as a performance criterion for the improved photoionization mass spectrometer because the detection of CO in air is of great practical importance and represents one of the most difficult cases. These difficulties were discussed in detail in the final report for Contract NAS1-4927 [1] where the previous detection limit of CO in N_2 at 0.5 percent was determined. But even this still high detection limit could only be obtained by using the nitrogen spark light source and by scanning the monochromator instead of the mass spectrometer. Figure 18 shows the result obtained with the instrument before improvement. The mass spectrometer was peaked at M = 28. With pure N_2 as sample gas, a defined structure of the background was still visible when the monochromator was scanned at wavelengths above the ionization wavelength of N_2. Particularly disturbing was a peak at 838Å which was caused by a second order line with a wavelength of 419Å. This peak is unfortunately very close to the only intense peak of the nitrogen spark light source at 835Å which could be used to ionize CO. The detection of 0.5 percent could only be accomplished by observing a slight distortion of the 838Å peak toward 835Å while the wavelength was scanned. It is clear that this kind of detection is far from ideal and too ambiguous; and if the Ar spark had been used, the detection limit would have been about one order of magnitude worse.

The use of a higher pressure in the Ar spark light source combined with the Ar gas filter and the improved electron deflector resulted in a significant improvement. A pressure of 200μ in the light source and of 500μ in the gas filter reduced the background due to residual ionization of N_2 by more than two orders of magnitude. Compared to N_2 the Ar spark provides more lines for the ionization, particularly the very prominent 879Å line which also yields a high photoionization cross section for CO. The result is demonstrated in the three lower traces of Figure 19. As one sees 0.05 percent of CO is now detected without any ambiguity and from the residual N_2 signal in the lowest pace, a detection limit of 100 ppm CO in N_2 can be extrapolated. It should be emphasized that this detection limit is now easily obtained by scanning the mass spectrometer while the monochromator is set for 879Å. Preliminary investigations, as demonstrated in Figure 20, no longer show any wavelength dependent structure in the residual ionization of N_2 between 800 and 900Å if the Ar filter and the higher pressure in the Ar spark source are used. The origin of the residual background and of a weak peak at 920Å is not yet known. Nevertheless, an improvement by more than a factor of 50 has been achieved and further improvement might be possible.

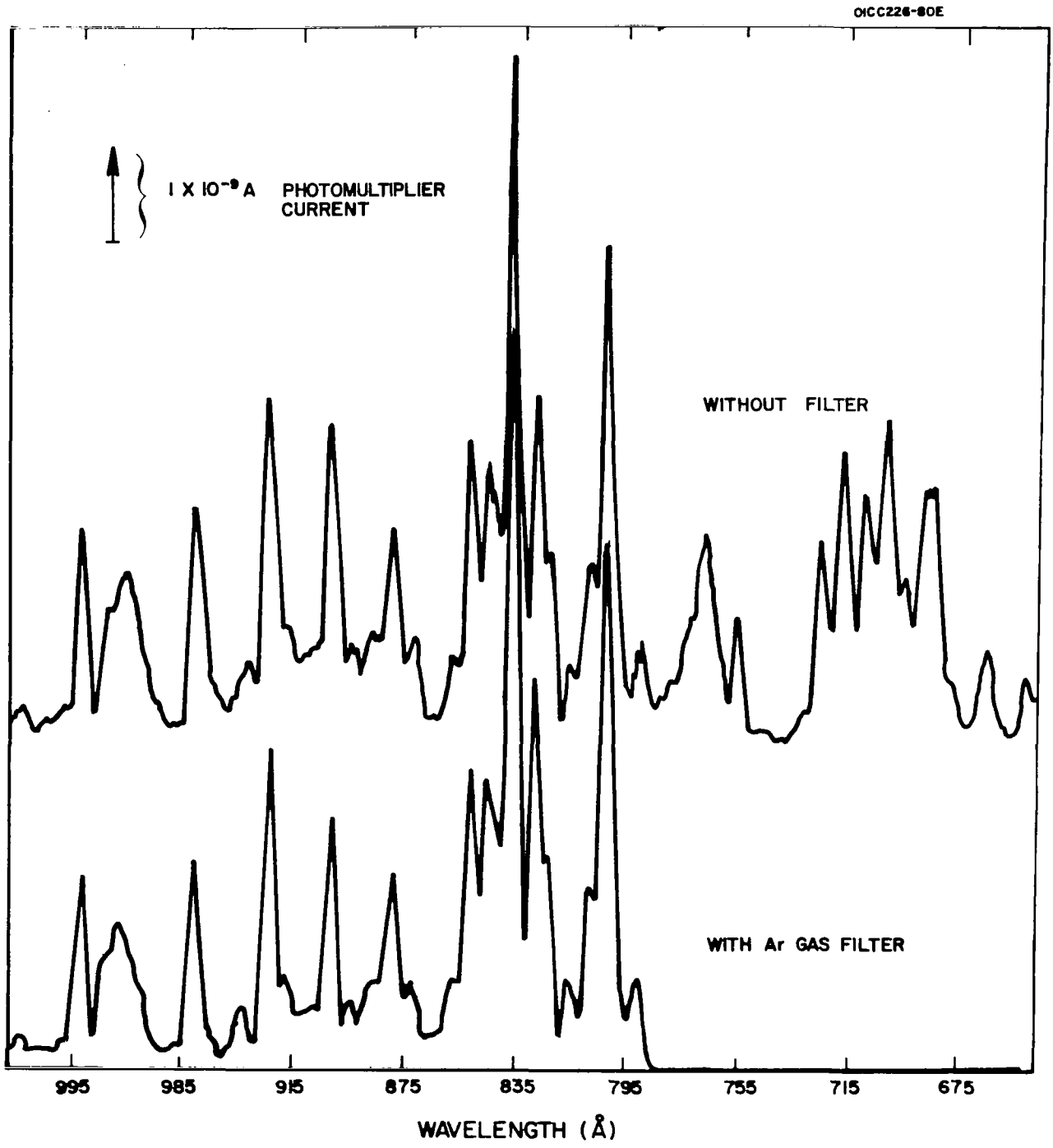

Figure 17. Spectrum of low pressure Ar spark source with and without Ar gas filter.

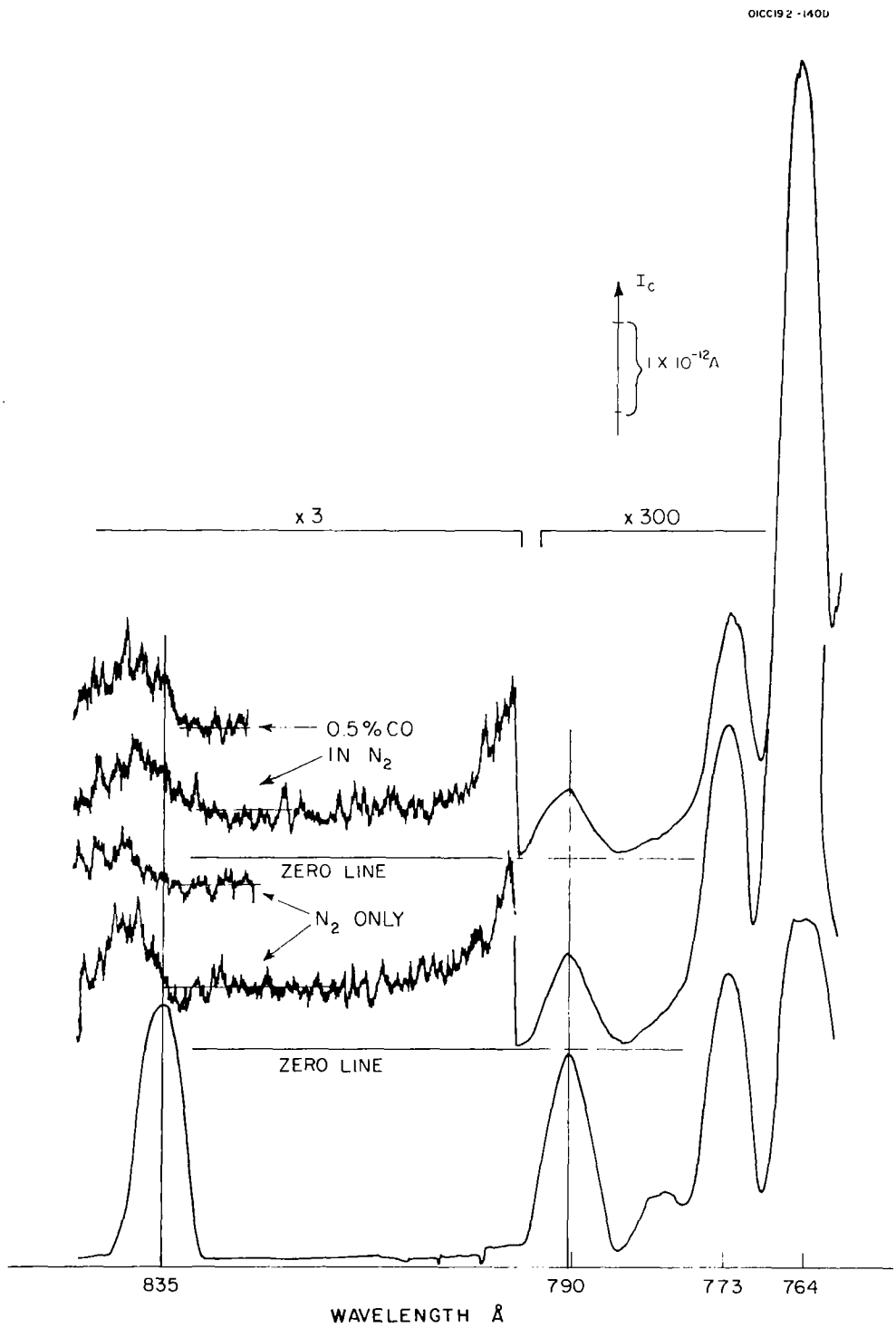

Figure 18. Detection of 0.5 percent CO in nitrogen.

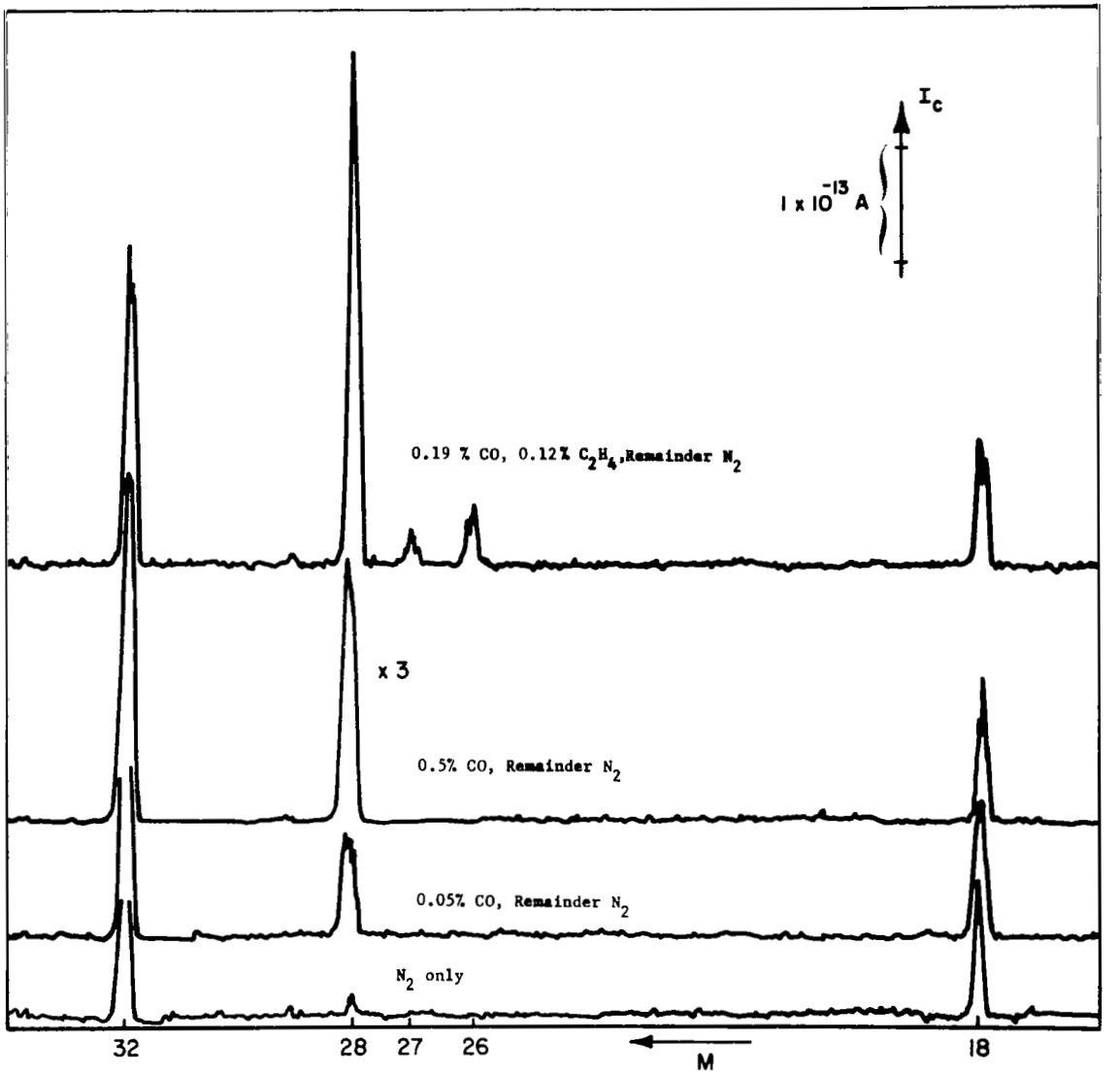

Figure 19. Detection of CO and CO + C_2H_4 in N_2.

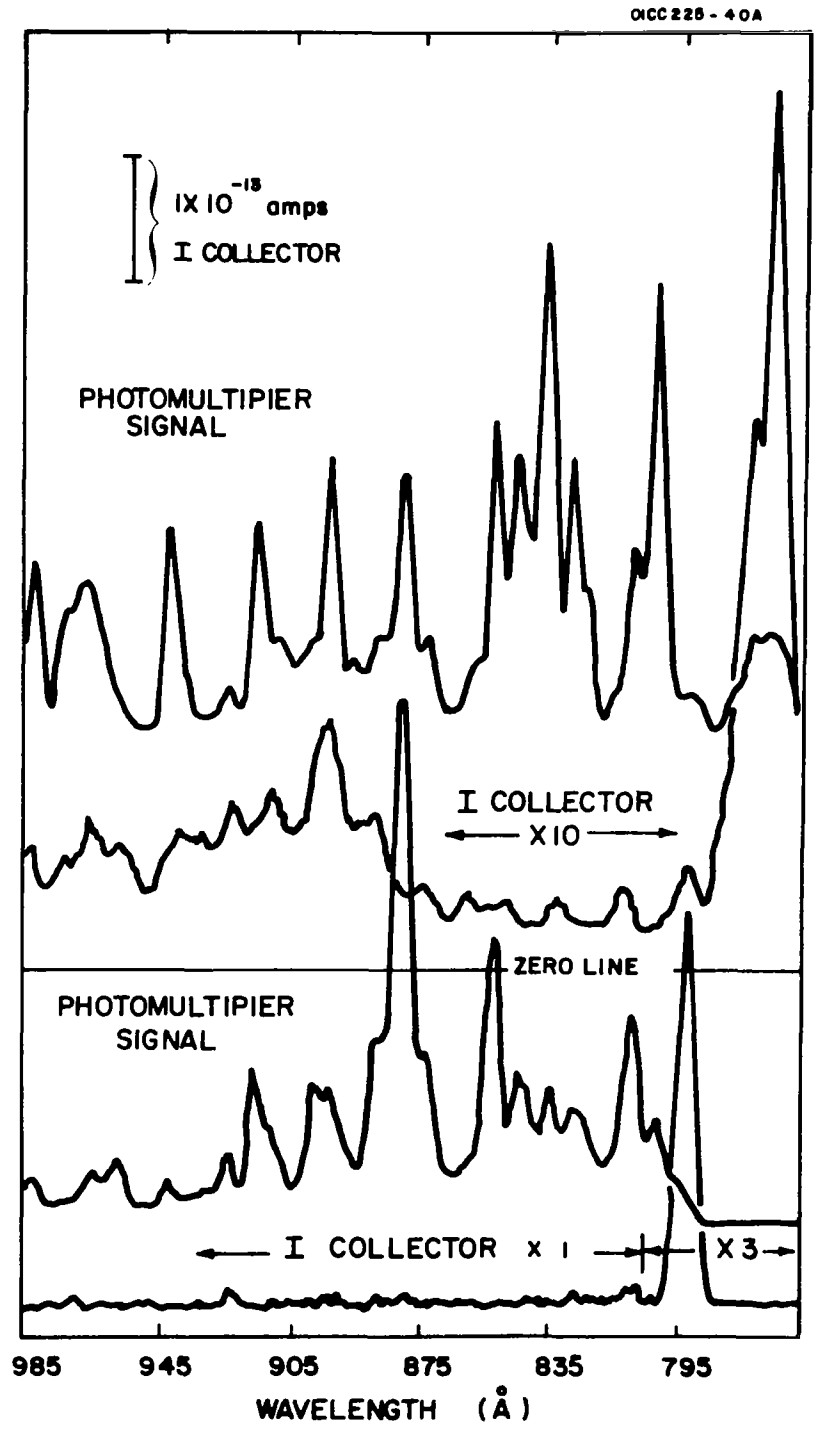

Figure 20. N_2 signal of M = 28 between 795 and 1000Å.

$CO - C_2H_4 - N_2$. It was of interest also to investigate a mixture of three gases with interfering mass peaks, since the amount of detectable CO also depends on the presence of other interfering compounds. Ethylene is such a compound, as its parent peak occurs on mass number 28. At a wavelength of 879Å, ethylene also fragments yielding signals on mass numbers 27 and 26. The relative signal strength was determined as 100:8.1:21.5 for mass numbers 28, 27 and 26, respectively, as found from a trace of pure ethylene. The trace of a mixture of 0.19 percent CO, 0.1 percent C_2H_4 and the remaining N_2 is shown in the upper trace of Figure 19. The amounts of ethylene can be assessed from the size of the 26 peak, and the amount of CO can be calculated by the difference from the mass 28 peak; but, in general, the lower limit for the detection of CO is given by the amount of ethylene present simultaneously. In this case, the detection limit of CO will be about 10 percent of the amount of C_2H_4 but not less than 100 ppm in the additional presence of N_2. In the calculation, one has to consider that ethylene shows about a 30 percent higher sensitivity than CO at 879Å. M = 26 is free of any interference in this mixture; therefore, a sensitivity limit for C_2H_4 of 50 to 100 ppm is obtained.

$N_2O - CO_2$. A mixture of 0.1 percent N_2O in CO_2 gives another example for the power of the photoionization mass spectrometer, since both gases produce a mass peak at M = 44. For the discrimination, a N_2 spark source was used in combination with the Ar gas filter. A strong line of the N_2 spark spectrum at 923Å was selected to ionize N_2O. Since the ionization onset of CO_2 is at 900Å, no ionization of CO_2 should occur. In this case, the detection limit was determined as 500 ppm. The sensitivity was limited by two reasons: N_2O has a comparatively low photoionization coefficient between its ionization threshold at 960Å and down to 900Å and the signal strength is reduced accordingly. In addition, the wavelength difference between the cutoff of the Ar filter at 800Å and the ionizing wavelength at 923Å is rather large, and all lines of the N_2 spark source in this range contribute to light scattering which results in residual ionization of some CO_2. Limitations in time did not permit improvement of this result, which seems to be possible by choice of a more suitable gas in the light source and in the gas filter. A Kr filter was tried with limited success, which may be caused by its fast decreasing absorption at shorter wavelengths. Here a mixture of Ar and Kr might be the solution.

Acetone - Butane. Both gases produce a parent peak at M = 58; the ionization potential of butane is 10.6 eV corresponding to 1160Å and that of acetone is 9.6 eV or 1280Å, respectively. Since an ionization wavelength between 1160 and 1280Å is required, an argon-hydrogen dc source was employed. The strong Lyman-α line at 1216Å was selected for this purpose. Argon was added to the discharge gas, since it suppresses the intensity of the molecular H_2 spectrum at shorter wavelengths. This measure, however, was not sufficient, and interference of scattered light was still obvious. The use of an Ar filter would not bring any improvement because the cutoff of the Ar filter is too far down. Considerable improvement was then achieved by using CO_2 in the gas filter. CO_2 assumes high absorption values below 1140Å as can be seen in Figure 9. A mixture of 0.17 percent acetone in butane was then analyzed and a detection limit of 100 ppm of acetone in butane was deduced.

Utilization of the Indium Filter. The filtering effect of the indium filter is demonstrated in Figure 21. The upper trace shows the unfiltered spectrum of the Ar spark source. (This spectrum shows some typical signs of air contamination in the Ar; compare with Figure 17.) The lower trace is the same spectrum with the indium filter applied. The sensitivity of the recording device was increased by a factor of 10 in order to compensate for the loss in transmittance. An increasing attenuation of wavelengths below 750Å is seen, and no transmission is visible below 650Å at the selected sensitivity. The transmittance also shows a decrease above 900Å, which is in agreement with the characteristics shown in Figure 2. A comparison of Figures 21 and 17 immediately reveals the inferiority of the indium filter, which is further discussed in the following.

The detection of CO in N_2 was again selected as the best test case for the performance of the indium filter, and the same mixture of 0.11 percent CO and remainder N_2 was used. In this case, the Ar spark source was run at low pressure in order not to suppress the short wavelengths already in the light source. Under these conditions, the 835Å line is stronger than the 879Å line and yields a somewhat better ionization. Figure 22 shows the result. The upper trace gives the residual background ionization of N_2 without any filter, the middle trace the same with the indium filter and the lowest trace was obtained with 0.11 percent CO in N_2. A detection limit of about 500 ppm can be deduced from these traces. The residual ionization was investigated for its wavelength dependence as demonstrated in Figure 23. The mass spectrometer was adjusted for M = 28, and then the monochromator was scanned from about 630 to 970Å. The photomultiplier gave the uv spectrum shown in Figure 21, while the signal from the ion multiplier was recorded simultaneously. Accordingly, the traces of both figures correspond to each other. Figure 23 again reflects the behavior of the indium filter, and a comparison with Figure 19 shows the differences with the Ar gas filter very well, particularly in the cutoff characteristics. The middle trace of Figure 21 does not indicate any strong wavelength dependent structure in the residual ionization, although again some increase of the background is observed around 915Å. A comparison with the lowest trace, which was obtained with the valve between the light source and monochromator closed, proves that the background is indeed caused by uv radiation and not by the noise of the recording multiplier and electrometer. The residual background, as obtained with the indium filter, is not significantly different from the residual background seen with the Ar gas filter; however, it must be emphasized that the signal strength in the range of transmittance of the indium filter is reduced by more than a factor of 10. The main drawback of the indium filter, therefore, lies mainly in the poor transmittance within its pass band and not so much in an insufficient cutoff characteristic.

It should also be mentioned that the proximity of the light source leads to a quick destruction of the indium filter. Prevention of this effect would necessitate setting the uv light source further back. It has already been pointed out earlier that an additional loss in light intensity would result from such a measure. The only other alternative location is in immediate proximity to the monochromator exit slit; this, however, would necessitate considerable changes in construction and it is uncertain whether other interferences would occur. It is felt that further investigations of the indium filter in this application is not warranted in light of the much better performance of the gas filter.

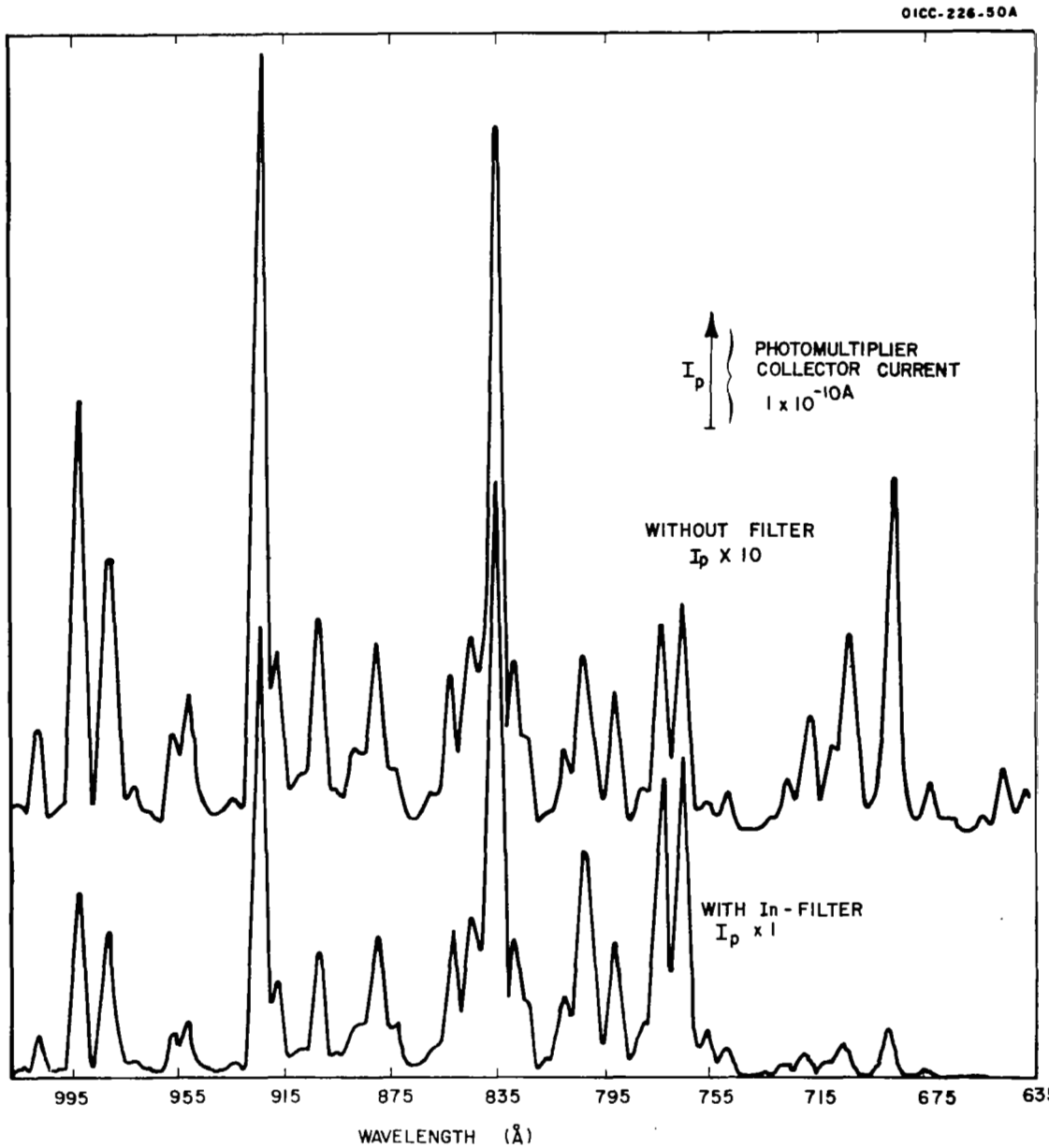

Figure 21. Spectrum of low pressure Ar spark source with and without In-filter.

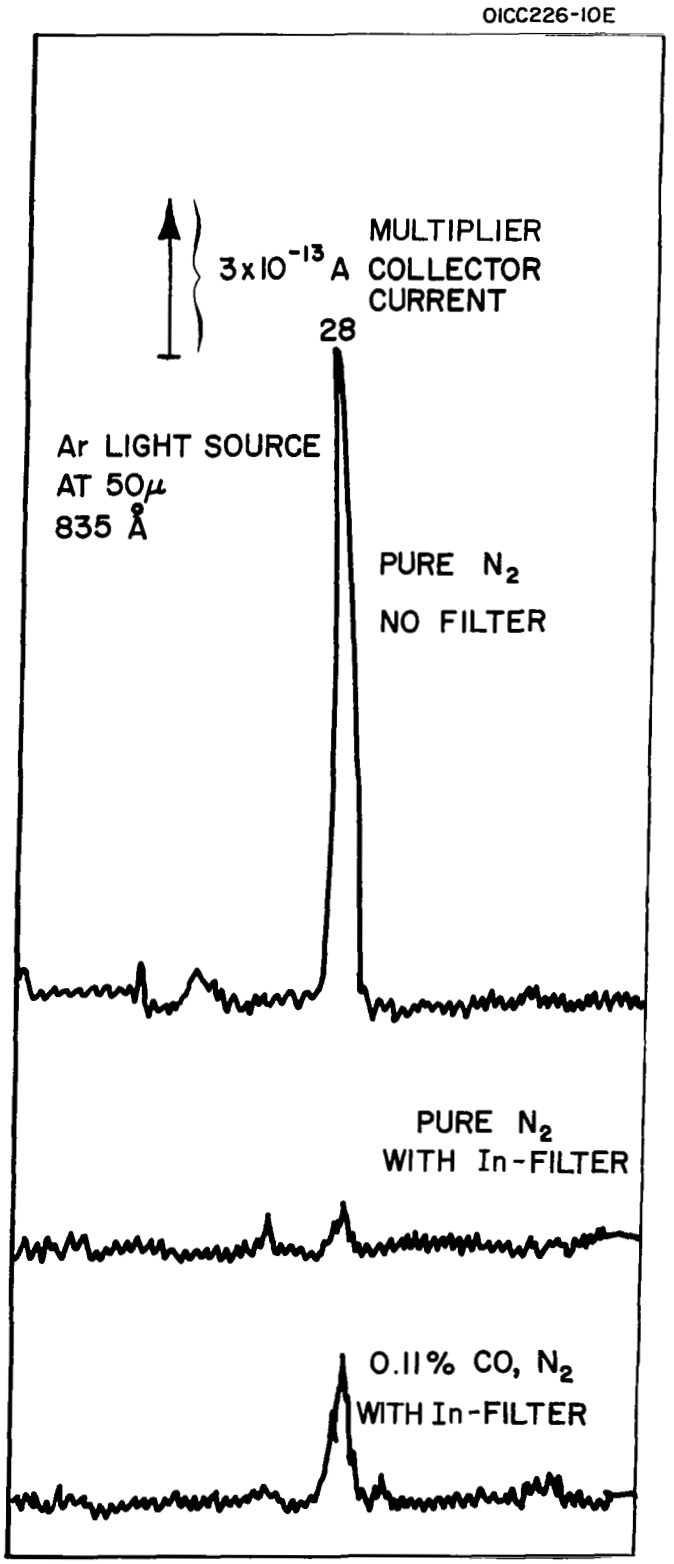

Figure 22. Detection of 0.11% CO in N_2 with In-filter.

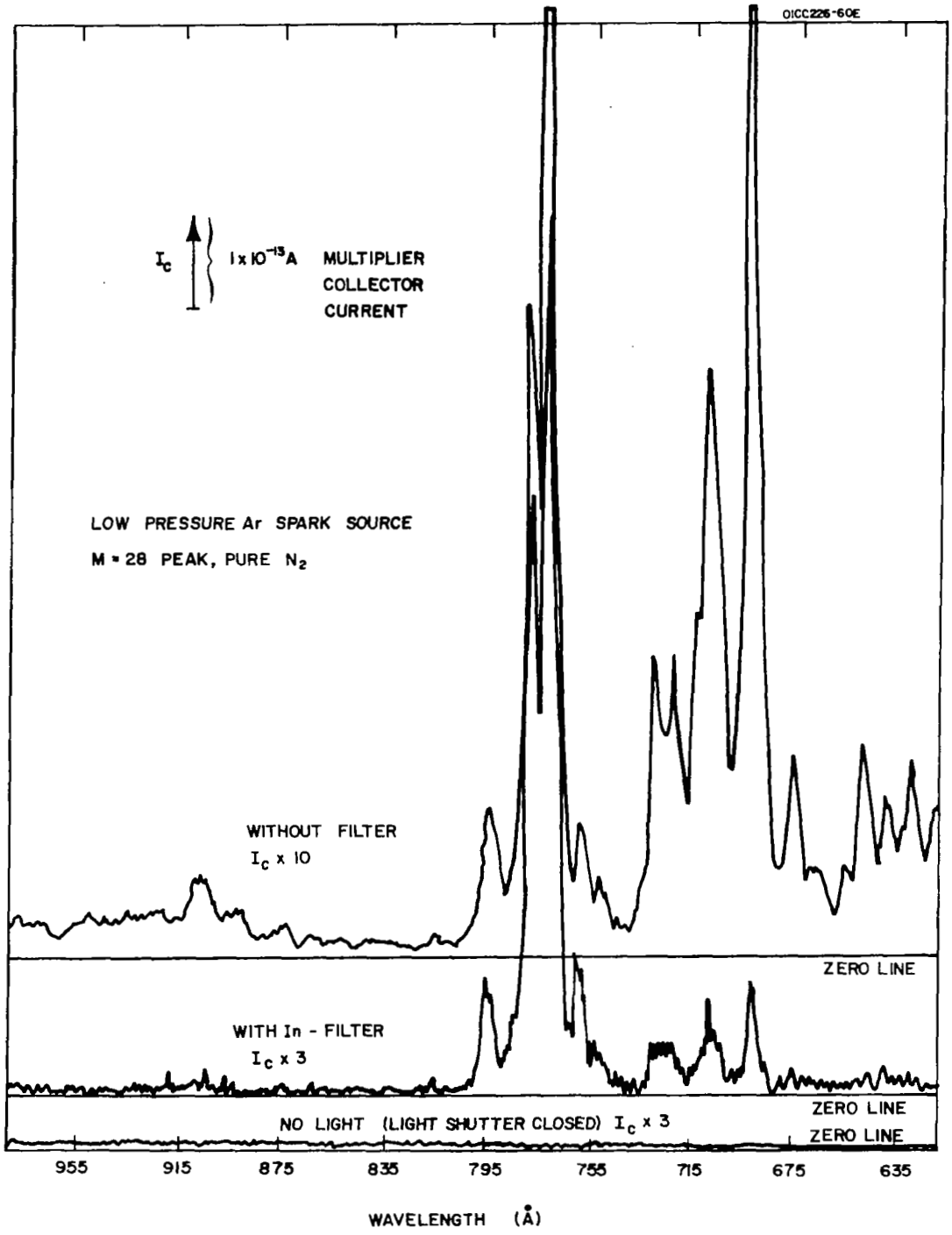

Figure 23. N_2 signal on M = 28 between 625 and 975Å.

CONCLUSIONS

The results achieved with the improved instrument are in very good agreement with the predictions made in the proposal which preceded this contract. The possibility of detecting 100 ppm of CO in N_2 without using high resolution mass spectrometry is an unique achievement of photoionization mass spectrometry. With a sensitivity between 10 and 100 ppm for gases without interfering mass peaks and with all the additional advantages of photoionization mass spectrometry. the field is opened for a wide analytical application. This contract concentrated on the detection of gases with interfering mass peaks because the original instrument was mainly disappointing in this respect; it also represents the most demanding task. By no means, however, is this the only advantage of this instrument. The cool ion source and the possibility of controlling dissociation of fragmentation is particularly valuable in the analysis of organic gases and vapors. If a certain complex molecule is ionized very close to the ionization threshold, fragmentation can be completely avoided, but with higher photon energies, more and more fragmentation will ensue. Theoretical considerations permit the prediction that the appearance and wavelength dependence of the cracking patterns will reveal isomer structures of such molecules. Certainly further research in this direction would be of great interest from a practical as well as from a theoretical point of view.

Further improvement of the basic sensitivity to better than 10 ppm seems to be quite feasible by application of a synchronous detection technique. The measurements indicate that the residual noise level is mainly caused by the statistical background current of the multiplier. If the spark source is used, light pulses of 1 to 2μ sec duration are produced at a rate of 120 per second. Consequently, also the ion current, arriving at the multiplier, is pulsed and it would only be necessary to register the multiplier signal during the length of these pulses. This can be achieved by using an electronic gate which is opened and closed in properly delayed synchronism with the light source pulses. If this gate is kept open for 8μ sec - which will sufficiently take care of the difference in the time of flight through the mass spectrometer - and the repetition rate is 120 per second, a duty cycle of 1/1000 results. This means that during one second, a total of only 1 millisecond is needed for sensing the actual signal. The statistical background signal, however, occurs completely at random and will be registered at its full average value by an integrating detection system without synchronous gating as it is presently used. Synchronous detection a duty cycle of 1/1000 should accordingly reduce the statistical background also by a factor of 1 1000. The increased sensitivity is not achieved by higher signal strength but by reduction of the background. A sensitivity below 10 ppm is based on the detection of only a few ions per second and the signal will show the corresponding statistical fluctuations; therefore, a longer integration time will be necessary for an accurate measurement. Very fast scanning with high accuracy is still beyond the capability of the photoionization mass spectrometer, but programmed recording of the mass range 1 to 50 in five minutes, with a sensitivity of 1 ppm, seems to be quite feasible.

An improvement of the general detection sensitivity will also permit further tracing of the sources causing the residual ionization when discriminative ionization is employed for the analysis of not mass-resolved doublets. Further improvement might be possible by the addition of a predispersing unit which will limit the bandwidth of light entering the monochromator to 50Å and which is designed especially to minimize loss of light intensity. In this way, the present detection limit of CO in N_2 of 100 ppm might be lowered to 10 ppm.

REFERENCES

1. Poschenrieder, W. P. and Barrington, A. F., "Development of a Mass Spectrometer Employing a Photoionization Source," GCA Technical Report No. 66-3-N, Contract No. NAS1-4927.

2. Hunt, W. R., Angel, D. W. and Tousey, R., "Thin Films and Their Uses for the Extreme Ultraviolet," Appl. Optics 4, 891 (1965).

3. Sullivan, J. O. and Holland, A. C., "Planetary Physics IX: A Congeries of Absorption Cross Sections for Wavelengths less than 3000Å," GCA Technical Report No. 64-20-N, Contract No. NASW-840.

4. Samson, J. A. R. and Kelley, F. L., "Planetary Physics III: Photoionization Cross Sections of the Rare Gases," GCA Technical Report No. 64-3-N, Contract No. NASW-840.

5. Samson, J. A. R., Techniques of Vacuum Ultraviolet Spectroscopy, John Wiley and Sons, Inc., publishers, New York, 1967.

6. Samson, J. A. R., "Planetary Aeronomy V: Vacuum Ultraviolet Light Sources," NASA CR-17, September 1963.

7. Diels, K. and Jaeckel, R., Leybold Vacuum - Taschenbuch, Springer-Verlag, publishers, 1962.